X-551-71-5
PREPRINT

NASA TM X-65450

IMP-I
LAUNCH WINDOW ANALYSIS

BERNARD KAUFMAN
DANIEL P. MUHONEN

JANUARY 1971

GSFC
GODDARD SPACE FLIGHT CENTER
GREENBELT, MARYLAND

X-551-71-5

IMP-I LAUNCH WINDOW ANALYSIS

Bernard Kaufman
Daniel P. Muhonen

JANUARY 1971

Goddard Space Flight Center
Greenbelt, Maryland

CONTENTS

IMP-I LAUNCH WINDOW ANALYSIS

I. INTRODUCTION

The IMP-I orbit is very different from previous IMPs in that it is first inserted into a parking or preliminary orbit. This park orbit is circular and inclined about 28.3 to the equator. After remaining in this orbit for exactly one-half period, the second stage is re-ignited and later separated from the third stage which injects the satellite into the final highly eccentric orbit. Final injection occurs over the west coast of Australia with the apogee of the orbit occurring over the northern hemisphere (Reference 1).

II. ORBITAL AND SPACECRAFT REQUIREMENTS

The final orbit of IMP-I is of course determined by the mission objectives. These objectives are to study solar and cosmic radiation, the solar plasma, wave particle interaction, and interplanetary and outer magnetospheric electromagnetic and electrostatic wave characteristics.

In order to achieve these objectives, IMP-I will be launched from ETR into a highly eccentric orbit of about 30° inclination with an apogee radius of about 30 Earth radii. The orbital requirements also include the following constraints:

A. An orbital lifetime not less than three years.

B. A perigee altitude not less than the injection height, although this may be reduced to 200 km altitude above a spherical Earth if suitable launch times are not otherwise available.

C. A centerline-station vector angle within 55° to 125°. This is the angle between the spin axis (centerline) and the vector to any tracking station. The spin axis will be reoriented after the first apogee so that it is perpendicular to the ecliptic (pointing in the direction of the south ecliptic pole) and will maintain this orientation. The reason for this constraint is that there are -8 db and -10 db nulls in the antenna pattern in the regions bounded by centerline-station vector angles of less than about 40° and greater than 135°. Only low bit rate (800 bps) telemetry operation is possible in these null regions; however, the satellite is designed to operate nominally at 3200 bps (Reference 2).

D. Ecliptic plane apogee-sun angle between 15° and 60° and decreasing with time. This angle is defined as the angle between the sun line from the Earth and the projection of the apogee vector from Earth onto the ecliptic plane. This will allow the projected apogee vector to go through the subsolar point between approximtely 15 and 60 days after injection.

E. The spin axis-sun angle from injection up to the first apogee must be known so that the spin axis may be reoriented to be perpendicular to the ecliptic. During this first half-orbit the spin axis is defined as the initial velocity vector at injection.

F. The spin axis-earth angle must be known up to the first apogee where reorientation of the spin axis will begin.

III. INJECTION CONDITIONS

The final earth-fixed injection conditions along with the estimated injection covariance matrix are shown in Table I. This information is taken from Reference 3.

IV. COMPUTING TECHNIQUES

A total of 20 hours of 360/95 computer time was required for this study. Many different computer programs were used and various checks were made during the course of the study by using independent programs to insure the accuracy of the results. The programs included both approximate and highly accurate numerical integration techniques. A brief description of each is probably in order.

A. SABAC

SABAC was developed by Renard and Sridharan (References 4 and 5) and uses approximate stability criteria which allow one to eliminate costly and time-consuming numerical integration. The rapidity of this program allows one to map out a complete launch window in a single computer run of less than two minutes, whereas use of numerical integration techniques would require many hours. While this program is approximate and is not intended to be highly accurate, it provides an extremely useful picture of the launch window as a basis for more detailed study. This program was obtained from the IMP project office.

B. ENCKE N-Body Numerical Integration Program (ENCKE)

ENCKE is an accurate n-body numerical integration program which was developed and written by B. Kaufman. Using a reference ellipse and integrating only the variations from this ellipse, the program is very fast compared to other n-body programs and has proven to be very accurate. The disturbing function includes the following:

1. Gravitational potential of the central body described by a linear combination of zonal, sectorial and tesseral harmonics,

2. Point mass effects of other bodies,

3. Solar radiation pressure.

The program also calculates penumbra and umbra times for the spacecraft and was modified to compute the angles described in II C, D, E and F above. ENCKE was the major computational device used in this study. Unfortunately no documentation exists yet for this program.

C. Network Analysis Program (NAP)

NAP is a highly accurate numerical integration program developed by DBA Systems, Inc. (Reference 6). Using power series methods, the program integrates the equations of motion for a spacecraft and includes in the model the following perturbations:

1. Gravitational potential described by a linear combination of zonal, sectorial and tesseral harmonics,

2. Point mass effects of other bodies,

3. Atmospheric drag,

4. Solar radiation pressure.

Since NAP was the only accurate program used which contained atmospheric drag, it was used mainly as a backup program to provide confidence in the results obtained from the faster Encke program described above.

D. Special Purpose Programs

Several special purpose programs were written to allow the calculation of contours of constant value for several of the angles discussed above. These contours will be discussed later.

V. LAUNCH WINDOW

A. Injection Times

Since the spacecraft will initially be inserted into a circular park orbit for exactly one-half period, all times mentioned in this report will be injection times into the final orbit. The actual liftoff times are found by taking into consideration the half-period of the park orbit.

Figure 1 (produced in part by SABAC) is a complete picture of the injection times from Jan. 15, 1971, to April 30, 1971, which yield a lifetime of at least three years. Various parts of this contour were chosen as test points in the Encke program and it was found that the contour was fairly accurate until approximately March 16, 1971, near 1600 to 1800 hours, where some complex forces apparently are beginning to combine in a manner that SABAC may not consider. As can be seen by the points plotted on the curve, this complex action is most significant around March 26 and appears to be disappearing at about April 10 and therefore is probably a cyclic occurrence related to the Sun. For this reason, if the launch is to occur later than about March 24, extreme care must be used. Several points plotted on Jan. 27 show just how sensitive the lifetime is to injection time where a difference of $1^h\ 15^m$ in injection time means the lifetime decreases from more than 3 years to about 4 days! Despite the above-mentioned complexities, Figure 1 is an excellent starting base for a detailed look at the launch window.

Superimposed on Figure 1 are two grids or contours: constant centerline-Earth angle, and ecliptic plane apogee-sun angle. The line of 0° for ecliptic plane apogee-sun angle was added in order to extend the window beyond March 30. The centerline-Earth angle is calculated at apogee (where the satellite spends the majority of its time) where the difference between it and the centerline-station angle is small.

Using the information available on Figure 1, it is seen that the window closes on March 30 if the ecliptic plane apogee-sun angle is not allowed to go below 15°. However, as discussed earlier this is precisely in the region where 3-year lifetimes may not exist. By lowering this constraint to 0°, the window extends

to April 11 but again the lifetime constraint is still somewhat cloudy here and would need detailed investigation by means of numerical integration. As can be easily seen, the centerline-Earth angle imposes no additional problems and the injection times are bounded by 1600 to about 1900 hrs. at the beginning and by 1600 to about 1800 hours near the end of the window.

B. Effect of Injection Errors on the Launch Window

The uncertainty in the state vector at injection is described by the injection covariance matrix in Table I. Because the off-diagonal terms are of significant magnitude, it was decided that it would be inadequate to examine only the effect of 3-sigma perturbations defined by the diagonal elements of the covariance matrix. Hence a Monte Carlo procedure was devised where a set of random state vectors was generated having a normal distribution about the nominal, as defined by the covariance matrix. The procedure involved the following steps:

1. Performing a coordinate rotation on the covariance matrix such that the resulting matrix was diagonal.

2. Generating 350 normally distributed random vectors, the elements of which had means zero, and variances equal to the elements of the diagonal matrix.

3. Multiplying these random vectors by the inverse rotation matrix and adding the nominal injection vector to each of the 350 resulting vectors.

These final 350 random vectors were then converted into the SABAC input coordinate system, and 350 corresponding launch windows were generated for each launch day considered. Details of the mathematics involved can be found in Appendix A.

It was originally planned to make runs using larger samples for some of the more desirable launch dates, but all the results using a sample size of 350 consistently showed that the launch window is essentially insensitive to injection state errors. Figures 2 and 3 show histograms of the lower and upper limits of the launch window on each Wednesday, January through April, 1971. The SABAC runs were made with lifetime studies at 15-minute intervals. In all cases, the launch window lower limit differed by no more than ±15 minutes from that of the nominal state vector, and over 99% of the upper limits were within 30 minutes of the nominal. The conclusion is that raising the nominal lower limit by fifteen minutes and lowering the nominal upper limit by 30 minutes should avoid any problems caused by injection state errors.

VI. SPACECRAFT PARAMETERS

A. Centerline-Station Vector Angle

Figures 4, 5, and 6 are curves of the maximum centerline-station vector angle and centerline-Earth angle for one period of a nominal orbit on three different launch dates. Table II represents the same data in tabular form and also shows the maximum difference between the two. It is seen that, after about 16 hours from injection, the difference between looking at the center of the Earth and at a station is less than 2° and that the angle is above the 55° lower boundary.

Figures 7 and 8 show a history of the centerline-Earth and maximum centerline-station angle as well as the angle to that station with the maximum deviation from the centerline-Earth angle. With the rate of increase seen here, the upper boundary of 125° will not be reached within the 3 years of the satellite's lifetime.

Table III shows the injection times for centerline-Earth angles at apogee from 55° to 85° from Jan. 27 to April 7, 1971. This data was used in superimposing the grid on Figure 1.

B. Ecliptic Plane Apogee-Sun Angle

As shown in Figure 1, the ecliptic plane apogee-sun angle imposes a tight constraint on the injection times, causing a closing of the window on March 30, 1971, if the angle is to be no lower than 15° at the first apogee. By allowing this constraint to drop to 0°, the window may be extended to April 11.

Table IV shows the ecliptic plane apogee-sun angle at the first apogee for 1/2-hour intervals across the injection window for a three-year lifetime. These data are presented weekly from Jan. 20 to April 28. Wednesdays were chosen as the typical injection dates solely for convenience and represent no special importance.

C. Spin Axis-Sun Angle

Table V shows the spin axis-sun angle from injection up to the first apogee in 4-hour intervals. These data are presented for every Wednesday from Jan. 27, 1971, to April 7, 1971, at the injection times which yield an ecliptic plane apogee-sun angle of 15°, 30°, 45°, and 60° and is within the three-year lifetime constraint. These two dates are for a 0° angle only. The spin axis is here assumed to be the initial velocity vector (inertial). At the first apogee, reorientation of the spin axis is begun.

D. Spin Axis-Earth Angle

The initial orbit has the same relationship with the rotating Earth regardless of the day or time of day on which injection occurs. Therefore the spin axis-Earth angle is invariant with respect to time, at least during the first half-orbit when perturbations have not yet altered the orbit. The spin axis is here again defined to be the initial velocity vector. This angle will start at 90° at perigee, increase to 180° at a true anomaly of 90° and then decrease to 90° at apogee.

Table VI shows the variation in the spin axis-Earth angle every two hours up to the first apogee where reorientation of the spin axis begins. The angle will of course change rapidly near perigee and Table VI shows that most of the change takes place in the first two hours. Figure 9 is a plot of the spin axis-Earth angle during these two hours.

VII. CHARACTERISTICS OF THE ORBIT

A. Perigee Radius

The lifetime of the spacecraft is accurately predicted by the behavior of the perigee radius. When perigee decreases sufficiently to allow the spacecraft to enter the atmosphere, then the effective life of the spacecraft is over since impact will occur shortly thereafter.

Figures 10 through 25 are plots of the periapsis radius every five orbits for three years. These plots are for an injection date of every Wednesday from January 27, 1971, through March 17, 1971, and for times on these days when the ecliptic plane apogee-sun angle is 15°, 30°, 45° and 60° where these times also satisfy the three-year lifetime constraint. From March 24 through April 7, the plots are for an angle of 0° in order to extend the window.

All of these curves were produced from runs made with the previously described Encke n-body program where the perturbations used included the presence of the sun and moon and a potential model for the Earth's asphericity. All of the runs were also checked for the first two months of the orbit on the NAP program using atmospheric drag to insure that the omission of drag did not affect the results. As can be seen from the curves, the perigee radius grows rapidly during the first few orbits and therefore the effects of drag (if any) will appear early. It was found that there were no noticeable atmospheric effects on the orbits.

B. Shadow Periods

At the top of Figures 10 through 25 are shown (by dark blocks) the orbits during which the spacecraft is in the shadow of either the Earth or the moon; however, due to the distance from the moon and the fact that only the penumbra of the moon's shadow is encountered, the latter is probably of no importance. Just below these blocks are two numbers indicating the maximum time spent in penumbra and umbra, respectively, during the entire interval when shadow occurs. Where only one number appears it indicates that only penumbra is encountered. The first block of shadow is always at or near perigee and the second block is near apogee.

C. World Map

Figures 6 and 7 are world maps or ground traces of the first two orbits for a typical nominal orbit. Table VII represents the same data in tabular form with the value of true anomaly also included.

ACKNOWLEDGMENTS

The authors wish to thank Mr. Raul Garza-Robles of GSFC for his help in making all the backup runs using the NAP program.

REFERENCES

1. Memo from Stephen J. Paddock, IMP Project Office. Subject: Request for Launch Window for IMP-I dated June 8, 1970.

2. Memo to R. E. Coady from S. J. Paddock, "IMP-I Launch Window Restraint, Centerline-Station Vector Angles," dated October 20, 1970.

3. Memo from S. J. Paddock, IMP Project Office. Subject: IMP-I Orbit Error Analysis, dated 28 August 1970.

4. Renard, M. L., "Approximate Stability Criteria for Highly Eccentric Orbits About the Earth," Preprint IAF-AD-83, 19th Int. Astron. Congress, New York, N.Y., October 13-19, 1968.

5. Renard, M. L., Sridharan, R., "Launch Window of a Highly Eccentric Satellite in an Orbit Normal to the Ecliptic," paper presented at the 9th Semi-annual Astrodynamics Conference NASA, GSFC, Greenbelt, Md., April 21-22, 1969.

6. Hartwell, J. G., Lewis, T. R., "Mathematical and Programming Documentation of a General Purpose Integrator Using Power Series Methods," prepared for NASA Langley Research Center. Contract #NAS1-9389, December 1969.

APPENDIX A

Monte Carlo Procedure for Study of Injection Errors

Assume that the injection covariance matrix, P, describes a normal distribution of injection state vectors, $\vec{X}_i$, having mean, $\vec{\tilde{X}}$, the nominal injection state vector. Then by definition

$$E(\vec{X}_i) = \vec{\tilde{X}}$$

$$E[(\vec{X}_i - \vec{\tilde{X}})\,(\vec{X}_i - \vec{\tilde{X}})^T] = P$$

where $E(x)$ denotes the expected value of x. Let S represent a coordinate rotation matrix, and suppose Q is the corresponding covariance matrix for $S\vec{X}_i$ about mean $S\vec{\tilde{X}}$. Then

$$Q = E[(S\vec{X}_i - S\vec{\tilde{X}})\,(S\vec{X}_i - S\vec{\tilde{X}})^T]$$

$$= E\{[S(\vec{X}_i - \vec{\tilde{X}})]\;[S(\vec{X}_i - \vec{\tilde{X}})]^T\}$$

$$= E[S(\vec{X}_i - \vec{\tilde{X}})\,(\vec{X}_i - \vec{\tilde{X}})^T\,S^T]$$

$$= SE[(\vec{X}_i - \vec{\tilde{X}})\,(\vec{X}_i - \vec{\tilde{X}})^T]\,S^T$$

$$= SPS^T$$

It is desired, if possible, to find a rotation matrix, S, such that Q is diagonal. If R is the matrix of eigenvectors for P, with associated eigenvalues, λ_i, then R^T will satisfy these properties. This is clear because

$$R^T P R = \text{diag.}\ (\lambda_i),$$

and R^T is a coordinate rotation matrix because it must be orthogonal.

The Monte Carlo procedure involves the following steps:

1. Scale the covariance matrix so that is will be better conditioned for evaluating the eigenvalues. Let P represent the scaled matrix, and let $\vec{\tilde{X}}$ represent the nominal state vector with the same scaling.

2. Evaluate the vector of eigenvalues, $\vec{\lambda}$, and associated matrix of eigenvectors, R, for the matrix P.

3. Generate a set of normally distributed random vectors, $\vec{\hat{X}}_i$, with mean $\vec{0}$ and variance $\vec{\lambda}$. These random vectors are in the coordinate system of $R^T \tilde{X}$.

4. Transform the random vectors to the $\vec{\tilde{X}}$ coordinate system, and add $\vec{\tilde{X}}$ to correct the mean:

$$\vec{X}_i = R\vec{\hat{X}}_i + \vec{\tilde{X}}.$$

5. Convert the random vectors $\vec{X}_i$ into the coordinate system and units acceptable by SABAC as input.

6. For each launch day of interest, run SABAC to generate a launch window for each of the $\vec{X}_i$ input vectors. The distribution of the limits of these launch windows on a given date describes the effect of injection errors on the launch window of that date.

Table I. Nominal State Vector and Covariance Matrix

INJECTION STATE VECTOR

1. ALTITUDE, ABOVE MEAN EQUATOR (km)	231.35075	
2. VELOCITY (km/sec)	10.806989	
3. FLIGHT PATH ANGLE (deg.)	0.	
4. FLIGHT PATH AZIMUTH (deg.)	73.5944	
5. LATITUDE (deg.)	-23.966	(SOUTH)
6. LONGITUDE (deg.)	111.449	(EAST)

COVARIANCE MATRIX

①	②	③	④	⑤	⑥
319.475	-.301558	-1.89925	3.06964	-1.85248	-7.01463
	.000314949	.00168757	-.00303874	.00174996	.00661598
		.0536598	-.0191042	.0116318	.0393667
			.0982999	-.0183223	-.0649491
				.0111156	.0392638
					.159351

Table II. Centerline - Station Angle/Centerline - Earth Angle

Time Epoch (hrs)	2/24/71 $17^h 0^m 47.5108$ ∢ from Center of ●	Max. Stat. ∢ Deviation	Distance from ● (Rm)	Max. Stat. ∢ (Deg.)	3/3/71 $17^h 3^m 16.5961$ ∢ from Center of ●	Max. Stat. ∢ Deviation	Distance from ● (Rm)	Max. Stat. ∢ (Deg.)	3/10/71 $17^h 6^m 29.5088$ ∢ from Center of ●	Max. Stat. ∢ Deviation	Distance from ● (Rm)	Max. Stat. ∢ (Deg.)
0			6,609				6,609				6,609	
1	41.8	12.9	22,766	54.7	42.2	12.8	22,765	50.0	43.1	12.7	22,765	55.8
2	40.5	6.5	37,585	47.0	42.1	6.5	37,585	48.6	44.2	6.3	37,585	50.5
3	41.8	4.5	49,900	46.3	43.9	4.4	49,900	48.3	46.4	4.3	49,900	50.7
4	43.2	3.4	60,638	46.7	45.5	3.4	60,637	48.9	48.2	3.3	60,637	51.5
5	44.4	3.1	70,253	47.3	46.9	2.9	70,253	49.7	49.7	2.8	70,252	52.3
6	45.5	3.2	79,000	47.8	48.1	3.1	79,000	50.4	50.9	3.0	79,000	53.2
7	46.4	3.3	87,058	48.7	49.1	3.2	87,057	51.2	51.9	3.2	87,058	54.0
8	47.3	3.3	94,528	49.4	50.0	3.3	94,526	52.0	52.9	3.3	94,529	54.8
9	48.0	3.3	101,497	50.0	50.7	3.3	101,494	52.7	53.7	3.3	101,458	55.6
10	48.7	3.3	108,027	52.0	51.4	3.3	108,023	54.8	54.4	3.4	108,028	57.8
12	49.9	2.9	119,952	52.7	52.7	2.9	119,945	55.1	55.7	2.9	119,954	58.5
14	50.9	2.5	130,588	53.1	53.7	2.5	130,577	55.9	56.7	2.5	130,590	58.9
16	51.8	1.9	140,127	53.4	54.7	1.9	140,111	56.2	57.7	1.9	140,130	59.3
18	52.6	2.4	148,709	55.0	55.5	2.4	148,686	57.9	58.5	2.4	148,712	60.9
20	53.4	2.3	156,435	55.7	56.3	2.3	156,405	58.6	59.3	2.3	156,439	61.6
22	54.1	2.1	163,387	56.2	57.0	2.1	163,346	59.1	60.0	2.1	163,391	62.1
24	54.7	1.8	169,625	56.6	57.6	1.8	169,572	59.5	60.7	1.8	169,629	62.5
26	55.3	2.0	175,200	56.9	58.2	2.0	175,133	59.8	61.3	2.0	175,203	62.8
28	55.9	1.8	180,151	57.2	58.8	1.8	180,006	60.1	61.9	1.8	180,154	63.1
30	56.5	1.1	184,512	57.5	59.4	1.1	184,411	60.4	62.5	1.1	184,514	63.5
32	57.0	1.3	188,310	58.0	59.9	1.3	188,183	60.9	63.0	1.3	188,311	64.0
34	57.6	1.7	191,567	58.5	60.5	1.7	191,420	61.5	63.5	1.7	191,565	64.5
36	58.1	1.8	194,300	59.9	61.0	1.8	194,126	62.8	64.1	1.8	194,294	65.9
38	58.6	1.6	196,524	60.2	61.5	1.6	196,319	63.1	64.6	1.6	196,514	66.2
40	59.1	1.6	198,250	60.4	62.0	1.6	198,011	63.3	65.1	1.6	198,234	66.4
42	59.6	1.6	199,487	61.2	62.5	1.6	199,210	64.1	65.6	1.6	199,463	67.2
44	60.1	1.8	200,240	61.9	63.0	1.8	199,921	64.8	66.1	1.8	200,208	67.9
(APOGEE) 46	60.6	1.8	200,514	62.4	63.5	1.8	200,147	65.3	66.5	1.8	200,471	68.3
48	61.1	1.7	200,310	62.8	64.0	1.7	199,891	65.6	67.0	1.7	200,255	68.7
50	61.6	1.6	199,628	63.1	64.5	1.7	199,150	65.9	67.5	1.6	199,557	69.0
52	62.2	1.7	198,463	63.4	65.0	1.7	197,922	66.3	68.1	1.7	198,374	69.3
54	62.7	1.1	196,812	63.7	65.5	1.1	196,200	66.6	68.6	1.1	196,702	69.7
56	63.2	1.1	194,666	64.2	66.0	1.1	193,976	67.1	69.1	1.1	194,532	70.1
58	63.8	1.5	192,015	64.8	66.6	1.5	191,239	67.6	69.6	1.5	191,853	70.7
60	64.4	1.9	188,845	66.3	67.2	1.9	187,973	69.1	70.2	1.9	188,651	72.1
62	65.0	1.8	185,135	66.8	67.8	1.8	184,163	69.6	70.8	1.8	184,909	72.6
64	65.7	1.7	180,877	67.2	68.4	1.7	179,785	70.0	71.4	1.7	180,606	73.0
66	66.3	1.5	176,034	67.6	69.1	1.5	174,813	70.3	72.1	1.5	175,715	73.4
68	67.1	1.8	170,577	68.8	69.8	1.8	169,214	71.5	72.8	1.8	170,204	74.3
70	57.9	2.2	164,468	70.1	70.5	2.2	162,946	72.7	73.5	2.2	164,035	75.7
72	68.7	2.2	157,660	70.9	71.4	2.2	155,961	73.6	74.3	2.2	157,158	76.7
74	70.0	2.1	150,094	71.8	72.3	2.2	148,193	74.3	75.2	2.1	149,512	77.4
76	70.7	2.3	141,695	72.7	73.3	2.4	139,564	75.3	76.2	2.3	141,021	78.3
78	71.9	1.9	132,365	73.8	74.5	1.9	129,968	76.4	77.4	1.9	131,584	79.3
80	73.3	1.9	121,975	75.2	75.9	1.9	119,264	77.8	78.7	1.9	121,067	80.6
82	75.0	2.3	110,347	77.0	77.6	2.4	107,254	79.6	80.3	2.4	109,284	82.4
84	77.2	3.1	97,222	79.5	79.7	3.3	93,649	82.2	82.4	3.2	95,964	84.9
86	80.1	4.0	82,195	83.1	82.7	4.2	77,980	86.0	85.2	4.1	80,676	88.4
88	84.5	5.4	64,564	89.8	87.5	5.8	59,394	93.3	89.5	5.4	62,658	94.9
90	92.9	8.0	42,843	100.9	97.6	9.6	35,927	107.2	97.9	8.4	40,243	106.3
92	129.7	15.6	12,659	128.4	91 hrs. 111.8	12.1	20,675	107.4	92 hrs. 137.6	24.8	8,540	140.3
(PERIGEE)→ 93	49.3	21.9	15,082	71.3	92 hrs. 87.8		7,376		93 hrs. 43.7	17.2	19,264	60.9

Table III. Centerline - Earth Angle at 1st Apogee
(After Reorientation of the Spin Axis)

INJECTION	CENTERLINE ANGLE			
	55°	65°	75°	85°
1/27/71	$17^h54^m35^s.745$	$19^h36^m55^s.527$	$21^h21^m20^s.843$	$23^h35^m21^s.086$
2/10/71	16 59 33 .012	18 41 52 .794	20 26 18 .110	22 40 18 .353
2/17/71	16 32 1 .646	18 14 21 .428	19 58 46 .743	22 12 46 .987
2/24/71	16 4 30 .280	17 46 50 .061	19 31 15 .377	21 45 15 .621
3/ 3/71	15 36 58 .913	17 19 18 .695	19 3 44 .011	21 17 44 .254
3/10/71	15 9 27 .547	16 51 47 .328	18 36 12 .644	20 50 12 .888
3/17/71	14 41 56 .180	16 24 15 .962	18 8 41 .278	20 22 41 .521
3/24/71	14 14 24 .814	15 56 44 .596	17 48 9..911	19 55 10 .155
3/31/71	13 46 53 .447	15 29 13 .229	17 13 38 .545	19 27 38 .788
4/ 7/71	13 19 22 .081	15 1 41 .863	16 46 7 .178	19 0 7 .422

Table IV. Ecliptic Plane Apogee - Sun Angle in 1/2 hour intervals

Note: Negative Angle Means Sun Leads the Apogee Vector
Positive Angle Means Sun Trails the Apogee Vector and Closes in Real Time

Date	Time	Angle (deg)
1/20/71	12h 00m	-81.8
	12 30	-73.0
	13 00	-63.8
	13 30	-54.2
	14 00	-44.3
	14 30	-34.2
	15 00	-24.0
	15 30	-14.0
	16 00	- 4.2
1/27/71	12h 00m	-80.9
	12 30	-71.7
	13 00	-62.1
	13 30	-52.2
	14 00	-42.1
	14 30	-32.0
	15 00	-21.9
	15 30	-12.1
	16 00	- 2.7
	16 30	6.3
	17 00	14.9
	17 30	23.0
	18 00	30.8
	18 30	38.3
	19 00	45.5
	19 30	52.4
	20 00	59.2
	20 30	65.9
	21 00	72.5
2/ 3/71	11h 00m	-97.4
	11 30	-88.7
	12 00	-79.6
	12 30	-70.0
	13 00	-60.1
	13 30	-50.1
	14 00	-39.9
	14 30	-29.9
	15 00	-20.0
	15 30	-10.6
	16 00	- 1.5
	16 30	7.1
	17 00	15.3
2/10/71	12h 00m	-77.9
	12 30	-68.1
	13 00	-58.0
	13 30	-47.8
	14 00	-37.8
	14 30	-27.9
	15 00	-18.4
	15 30	- 9.35
	16 00	± 0.7
	16 30	7.5
	17 00	15.4
	17 30	22.9
	18 00	30.1
	18 30	37.1
	19 00	43.9
	19 30	50.6
	20 00	57.2
2/17/71	11h 00m	-95.3
	11 30	-85.8
	12 00	-75.9
	12 30	-65.9
	13 00	-55.7
2/17/71	13h 30m	-45.7
	14 00	-35.8
	14 30	-26.3
	15 00	-17.2
	15 30	- 8.5
	16 00	± 0.2
	16 30	7.7
	17 00	15.2
	17 30	22.5
	18 00	29.5
	18 30	36.3
	19 00	43.0
	19 30	49.6
	20 00	56.1
2/24/71	11h 00m	-93.6
	11 30	-83.8
	12 00	-73.7
	12 30	-63.6
	13 00	-53.5
	13 30	-43.7
	14 00	-34.1
	14 30	-24.9
	15 00	-16.2
	15 30	- 7.9
	16 00	0.0
	16 30	7.6
	17 00	14.8
	17 30	21.8
	18 00	28.7
	18 30	35.4
	19 00	42.0
3/ 3/71	10h 00m	-110.8
	10 30	-101.4
	11 00	-91.7
	11 30	-81.6
	12 00	-71.5
	12 30	-61.4
	13 00	-51.5
	13 30	-41.9
	14 00	-32.7
	14 30	-23.9
	15 00	-15.6
	15 30	- 7.7
	16 00	± 0.1
	16 30	7.2
	17 00	14.2
	17 30	21.1
	18 00	27.8
3/10/71	11h 00m	-89.5
	11 30	-79.3
	12 00	-69.2
	12 30	-59.3
	13 00	-49.7
	13 30	-40.4
	14 00	-31.6
	14 30	-23.3
	15 00	-15.3
	15 30	- 7.6
	16 00	± 0.4
	16 30	6.7
	17 00	13.5
	17 30	20.3
	18 00	26.9
	18 30	33.5
	19 00	40.0
3/17/71	10h 00m	-107.3
	10 30	-97.3
	11 00	-87.1
	11 30	-77.0
	12 00	-67.1
	12 30	-57.4
	13 00	-48.2
	13 30	-39.3
	14 00	-30.9
	14 30	-22.9
	15 00	-15.3
	15 30	- 8.0
	16 00	± 0.9
	16 30	6.0
	17 00	12.7
	17 30	19.4
	18 00	25.9
3/24/71	10h 00m	-105.0
	10 30	-94.9
	11 00	-84.8
	11 30	-74.8
	12 00	-65.2
	12 30	-55.9
	13 00	-47.0
	13 30	-38.5
	14 00	-30.5
	14 30	-22.8
	15 00	-15.5
	15 30	- 8.4
	16 00	- 1.5
	16 30	5.2
	17 00	11.9
	17 30	18.5
	18 00	25.0
3/31/71	10h 00m	-102.7
	10 30	-92.5
	11 00	-82.6
	11 30	-72.9
	12 00	-63.5
	12 30	-54.6
	13 00	-46.1
	13 30	-38.1
	14 00	-30.4
	14 30	-23.0
	15 00	-15.9
	15 30	- 9.0
	16 00	- 2.2
	16 30	4.4
	17 00	11.0
	17 30	17.5
	18 00	24.1
4/ 7/71	10h 00m	-100.3
	10 30	-90.3
	11 00	-80.5
	11 30	-71.2
	12 00	-62.2
	12 30	-53.7
	13 00	-45.6
	13 30	-37.9
4/ 7/71	14h 00m	-30.5
	14 30	-23.4
	15 00	-16.4
	15 30	- 9.7
	16 00	- 3.0
	16 30	3.6
	17 00	10.1
	17 30	16.7
	18 00	23.2
4/14/71	09h 00m	-118.1
	09 30	-108.0
	10 00	-97.9
	10 30	-88.2
	11 00	-78.8
	11 30	-69.8
	12 00	-61.3
	12 30	-53.1
	13 00	-45.4
	13 30	-38.0
	14 00	-30.8
	14 30	23.9
	15 00	-17.1
	15 30	-10.4
	16 00	- 3.8
	16 30	2.7
	17 00	9.3
4/21/71	08h 00m	-135.9
	08 30	-125.8
	09 00	-115.6
	09 30	-105.6
	10 00	-95.8
	10 30	-86.4
	11 00	-77.4
	11 30	-68.8
	12 00	-60.6
	12 30	-52.9
	13 00	-45.4
	13 30	-38.2
	14 00	-31.3
	14 30	-24.5
	15 00	-17.8
	15 30	-11.2
	16 00	- 4.7
4/28/71	08h 00m	-133.4
	08 30	-123.3
	09 00	-113.3
	09 30	-103.4
	10 00	-94.0
	10 30	-84.9
	11 00	-76.3
	11 30	-68.1
	12 00	-60.3
	12 30	-52.8
	13 00	-45.6
	13 30	-38.6
	14 00	-31.8
	14 30	-25.2
	15 00	-18.6
	15 30	-12.0
	16 00	- 5.5

Table V. Spin Axis - Sun Angle (Deg) (spin axis is initial velocity vector)

INJECTION DATE - 1971

Time from Epoch (hrs)	1/27 $17^h0^m25^s.811$	1/27 $17^h56^m43^s.628$	1/27 $18^h58^m1^s.675$	2/10 $16^h58^m30^s.896$	2/10 $17^h59^m33^s.469$	2/17 $16^h0^m44^s.494$	2/17 $16^h59^m9^s.358$	2/17 $18^h2^m21^s.659$
0	97.9	85.0	71.4	97.7	83.5	110.9	97.0	82.1
4	98.1	85.2	71.5	97.9	83.6	111.1	97.1	82.2
8	98.2	85.3	71.7	98.0	83.8	111.2	97.3	82.3
12	98.4	85.5	71.8	98.2	83.9	111.4	97.4	82.5
16	98.5	85.6	71.9	98.3	84.0	111.5	97.6	82.6
20	98.7	85.7	72.1	98.5	84.2	111.7	97.7	82.8
24	98.8	85.9	72.2	98.6	84.3	111.8	97.8	82.9
28	99.0	86.0	72.3	98.8	84.4	111.9	98.0	83.0
32	99.1	86.2	72.5	98.9	84.6	112.1	98.1	83.2
36	99.2	86.3	72.6	99.0	84.7	112.2	98.2	83.3
40	99.4	86.5	72.7	99.2	84.8	112.4	98.4	83.4
44	99.5	86.6	72.9	99.3	85.0	112.5	98.5	83.5
APOGEE (46)	99.6	86.7	72.9	99.4	85.1	112.6	98.6	83.6

Time from Epoch (hrs)	2/24 $17^h0^m47^s.108$	2/24 $18^h5^m52^s.373$	3/3 $17^h3^m16^s.961$	3/10 $17^h6^m29^s.082$	3/17 $17^h10^m11^s.839$	3/24 $16^h6^m38^s.629$	3/31 $16^h10^m1^s.470$	4/7 $16^h13^m43^s.990$
0	95.8	80.3	94.2	92.4	90.3	104.4	102.4	100.2
4	96.0	80.5	94.4	92.5	90.5	104.6	102.5	100.4
8	96.1	80.6	94.5	92.7	90.6	104.7	102.6	100.5
12	96.2	80.7	94.7	92.8	90.7	104.8	102.8	100.6
16	96.4	80.9	94.8	92.9	90.9	105.0	102.9	100.8
20	96.5	81.0	94.9	93.1	91.0	105.1	103.0	100.9
24	96.6	81.1	95.1	93.2	91.1	105.2	103.1	101.0
28	96.8	81.3	95.2	93.3	91.2	105.4	103.3	101.1
32	96.9	81.4	95.3	93.5	91.4	105.5	103.4	101.3
36	97.0	81.5	95.5	93.6	91.5	105.6	103.5	101.4
40	97.2	81.6	95.6	93.7	91.6	105.7	103.6	101.5
44	97.3	81.8	95.7	93.8	91.8	105.9	103.8	101.6
APOGEE (46)	97.4	81.8	95.8	93.9	91.8	105.9	103.8	101.7 (Impact 1029 Days)

Table VI. Spin Axis - Earth Angle
(Spin Axis is Initial Velocity Vector)

Time from Epoch (hrs)	Angle (deg)	Time from Epoch (hrs)	Angle (deg)
0	90.0	24	98.9
2	135.2	26	97.9
4	122.5	28	97.0
6	116.4	30	96.1
8	112.5	32	95.3
10	109.6	34	94.4
12	107.3	36	93.6
14	105.4	38	92.9
16	103.8	40	92.1
18	102.4	42	91.3
20	101.2	44	90.6
22	100.0	APOGEE ≈ 46	89.9

Table VII. World Map: Injection 10 Feb. 1971 $16^h 58^m 30^s.899$

ECLIPTIC PLANE APOGEE - SUN ANGLE = 15° LONGITUDE IS POSITIVE EAST

LATITUDE { + NORTH, - SOUTH ANOMALY { + HEADING TOWARD APOGEE, - HEADING TOWARD PERIGEE

Time from Epoch	Lat. (deg)	Long. (deg)	True Anomaly (deg)	Time from Epoch	Lat. (deg)	Long. (deg)	True Anomaly (deg)
0^h	-24.0	111.4	0	$92^h 10^m$	-22.0	171.5	6.0
$0^h 2^m$	-20.4	122.4	11.2	$92^h 12^m$	-18.1	-178.4	16.7
$0^h 4^m$	-16.3	132.4	21.9	$92^h 14^m$	-13.8	-169.2	26.9
$0^h 6^m$	-12.0	141.3	32.0	$92^h 16^m$	- 9.6	-161.1	36.4
$0^h 8^m$	- 7.8	149.1	41.2	$92^h 18^m$	- 5.5	-154.0	44.9
$0^h 20^m$	9.9	179.0	78.4	$92^h 20^m$	- 1.8	-147.7	52.3
1^h	24.7	-152.5	117.9	$93^h 0^m$	23.8	-102.0	112.5
2^h	28.0	-149.0	134.8	94^h	28.2	- 95.0	132.7
10^h	28.0	120.0	160.8	100^h	28.5	-157.6	157.0
20^h	26.6	- 21.4	168.9	110^h	27.0	63.5	167.3
30^h	25.5	-166.3	173.8	120^h	25.8	- 80.9	172.8
40^h	24.5	47.5	177.8	130^h	24.7	133.1	176.9
46^h	23.9	- 40.4	180.0	138^h	23.8	16.0	179.9
50^h	23.5	- 99.0	-178.5	140^h	23.6	- 13.3	-179.3
60^h	22.2	114.6	-174.7	150^h	22.4	-159.8	-175.5
70^h	20.6	- 31.0	-169.9	160^h	20.9	54.4	-170.9
80^h	17.9	-174.2	-162.6	170^h	18.4	- 89.5	-164.4
90^h	6.0	59.9	-135.8	180^h	11.3	135.7	-147.6
$90^h 54^m$	0.0	57.4	-123.3	182^h	5.9	116.0	-136.0
91^h	- 1.1	57.8	-121.1	183^h	0.0	113.1	-122.2
$91^h 30^m$	- 9.5	65.8	-103.5	$183^h 30^m$	- 8.4	119.4	-106.5
$91^h 40^m$	-14.5	73.4	- 92.5	$183^h 40^m$	-12.6	125.1	- 97.4
$91^h 50^m$	-21.3	87.8	- 75.1	$183^h 50^m$	-18.4	135.7	- 83.5
$91^h 52^m$	-22.9	92.1	- 70.3	$183^h 52^m$	-19.8	138.7	- 79.9
$91^h 54^m$	-24.5	97.3	- 64.9	$183^h 54^m$	-21.2	142.3	- 75.8
$91^h 56^m$	-26.0	103.3	- 58.8	$183^h 56^m$	-22.8	146.4	- 71.3
$91^h 58^m$	-27.4	110.3	- 51.9	$183^h 58^m$	-24.3	151.2	- 66.2
$92^h 0^m$	-28.5	118.5	- 44.2	$184^h 0^m$	-25.8	156.8	- 60.9
$92^h 2^m$	-29.0	127.8	- 35.6	$184^h 2^m$	-27.2	163.3	- 50.1
$92^h 4^m$	-28.8	138.2	- 26.1	$184^h 4^m$	-28.3	170.8	- 46.8
$92^h 6^m$	-27.6	149.3	- 15.8	$184^h 6^m$	-29.0	179.5	- 38.8
$92^h 8^m$	-25.3	160.5	- 5.0	$184^h 8^m$	-29.0	-170.8	- 29.9
$92^h 10^m$	-22.0	171.5	6.0	$184^h 10^m$	-28.2	-160.3	- 20.2
				$184^h 12^m$	-26.4	-149.5	- 9.9
				$184^h 14^m$	-23.6	-138.7	0.6

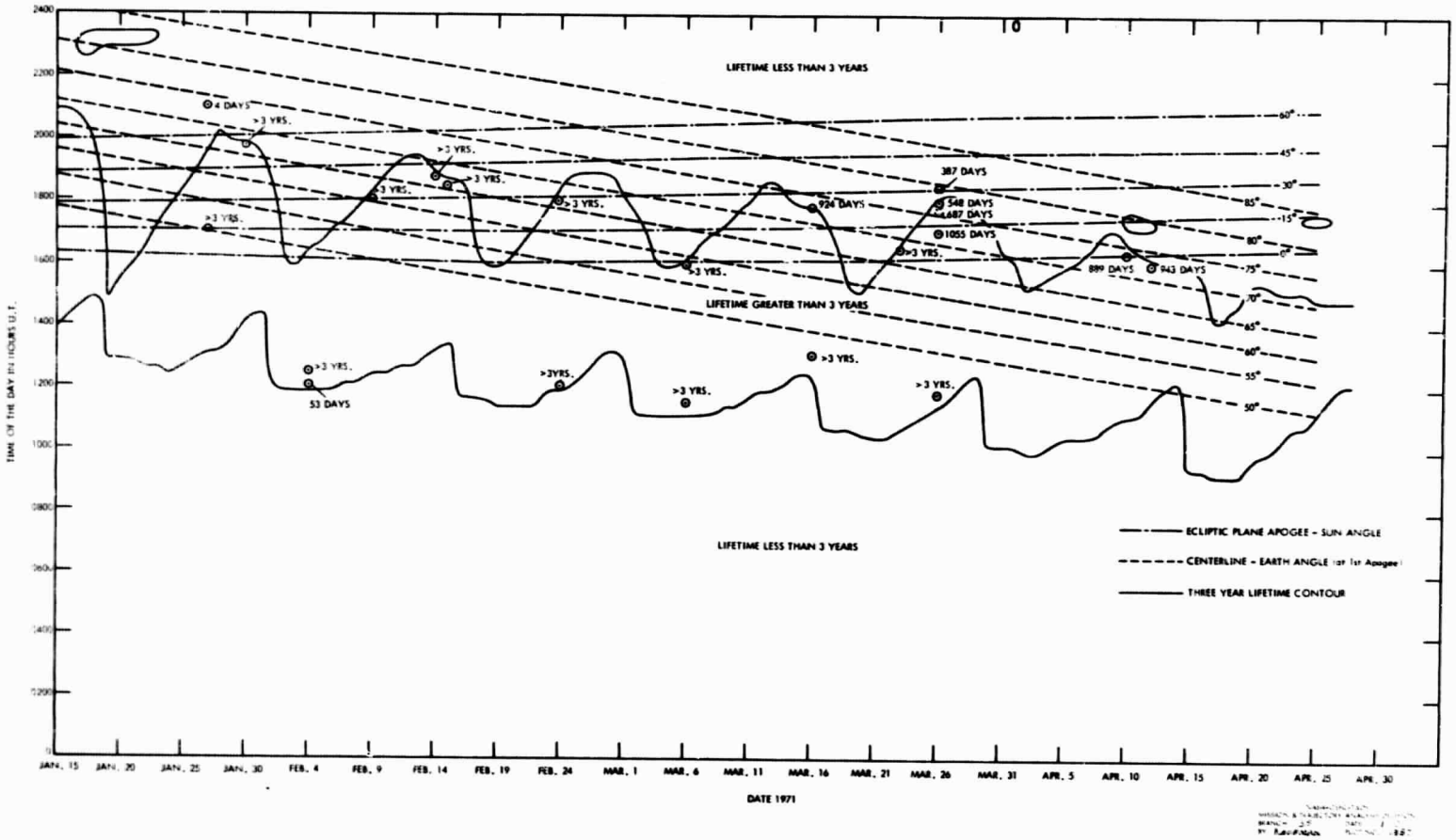

Figure 1. Nominal IMP-I Launch Window (0 km Initial Perigee Drop)

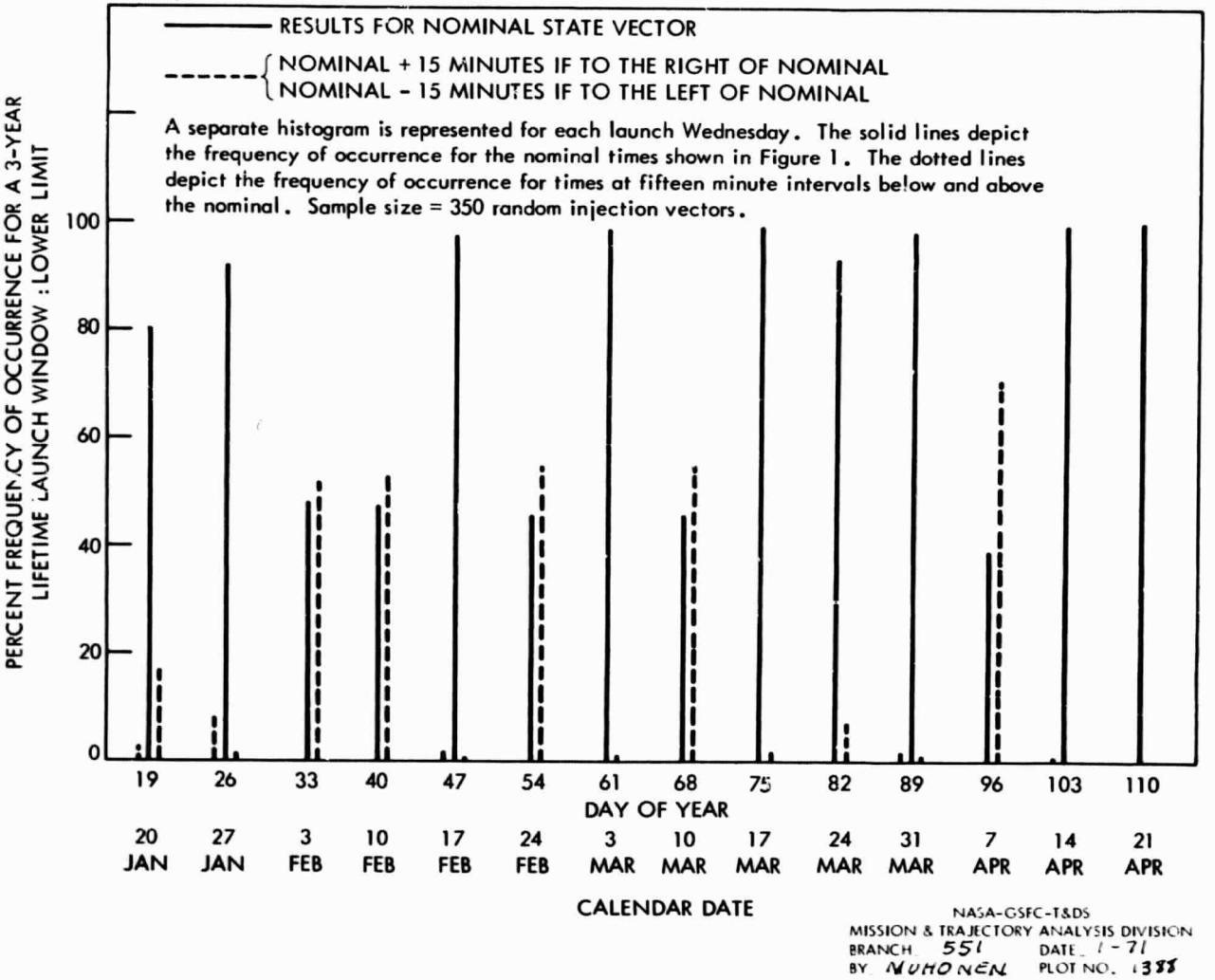

Figure 2. Histograms for Launch Window Lower Limits on each Wednesday Jan. - Apr. 1971

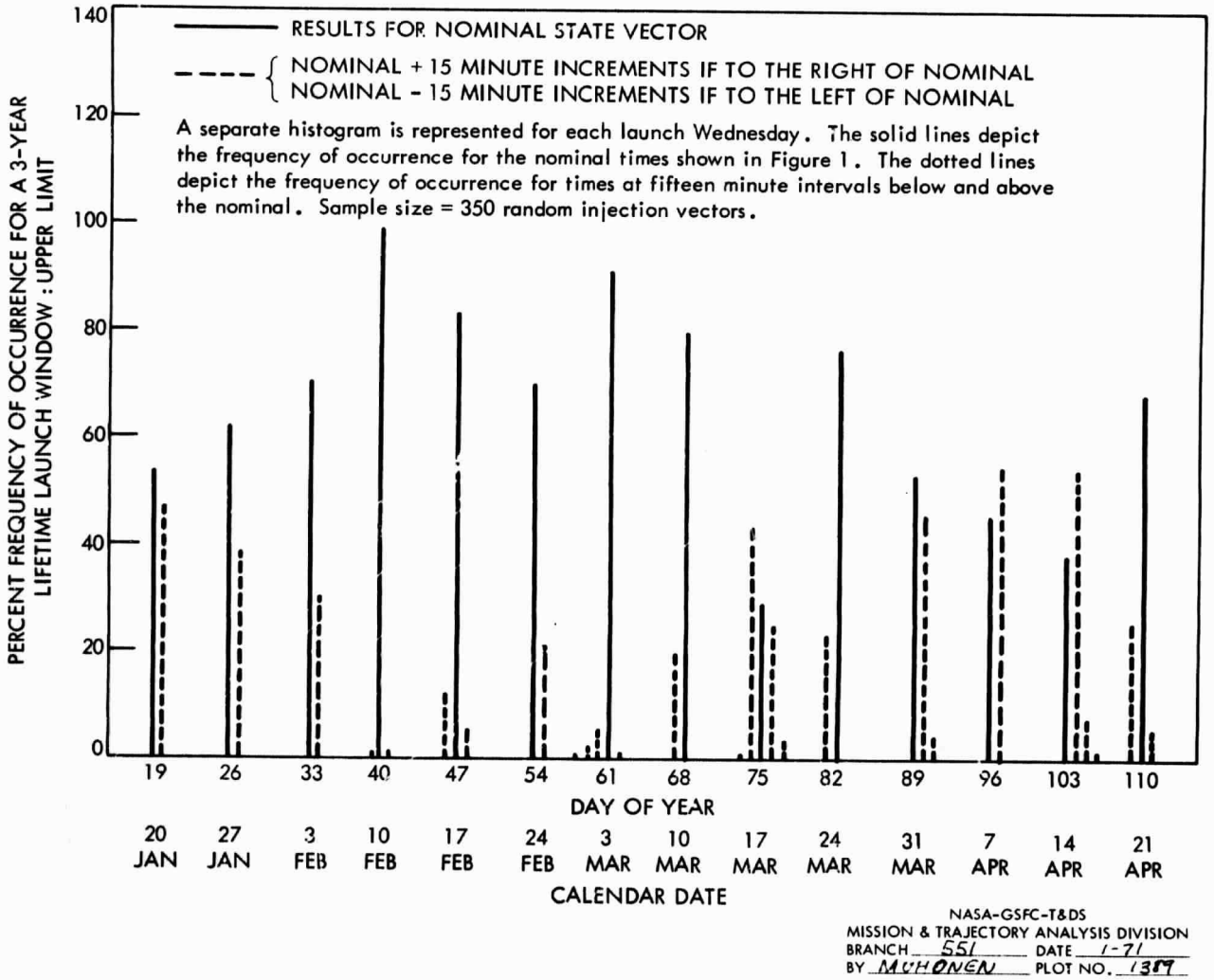

Figure 3. Histograms for Launch Window Upper Limits on each Wednesday Jan. - Apr. 1971

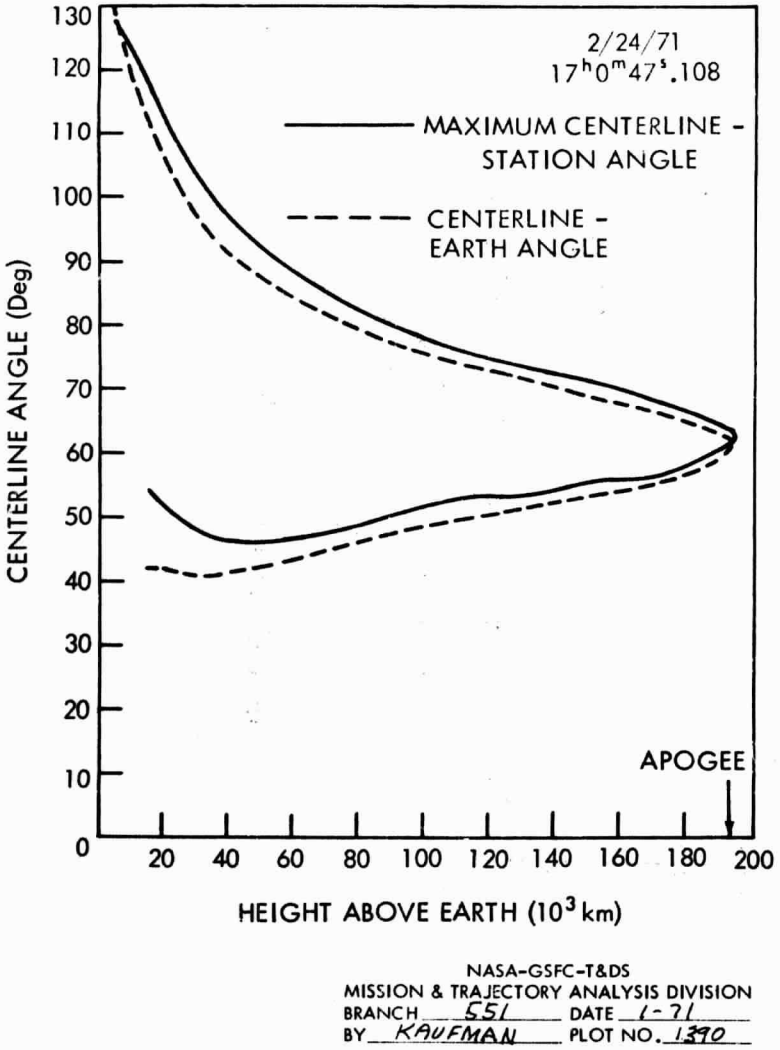

NASA-GSFC-T&DS
MISSION & TRAJECTORY ANALYSIS DIVISION
BRANCH 551 DATE 1-71
BY KAUFMAN PLOT NO. 1390

Figure 4. Centerline Angle

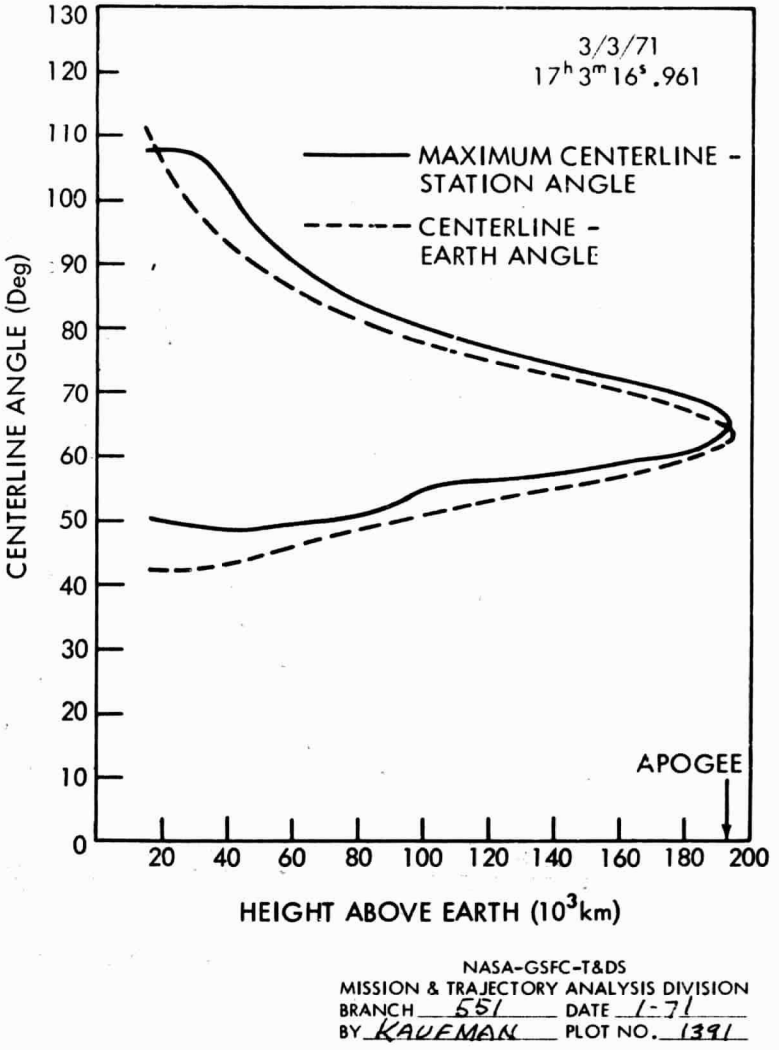

NASA-GSFC-T&DS
MISSION & TRAJECTORY ANALYSIS DIVISION
BRANCH 551 DATE 1-71
BY KAUFMAN PLOT NO. 1391

Figure 5. Centerline Angle

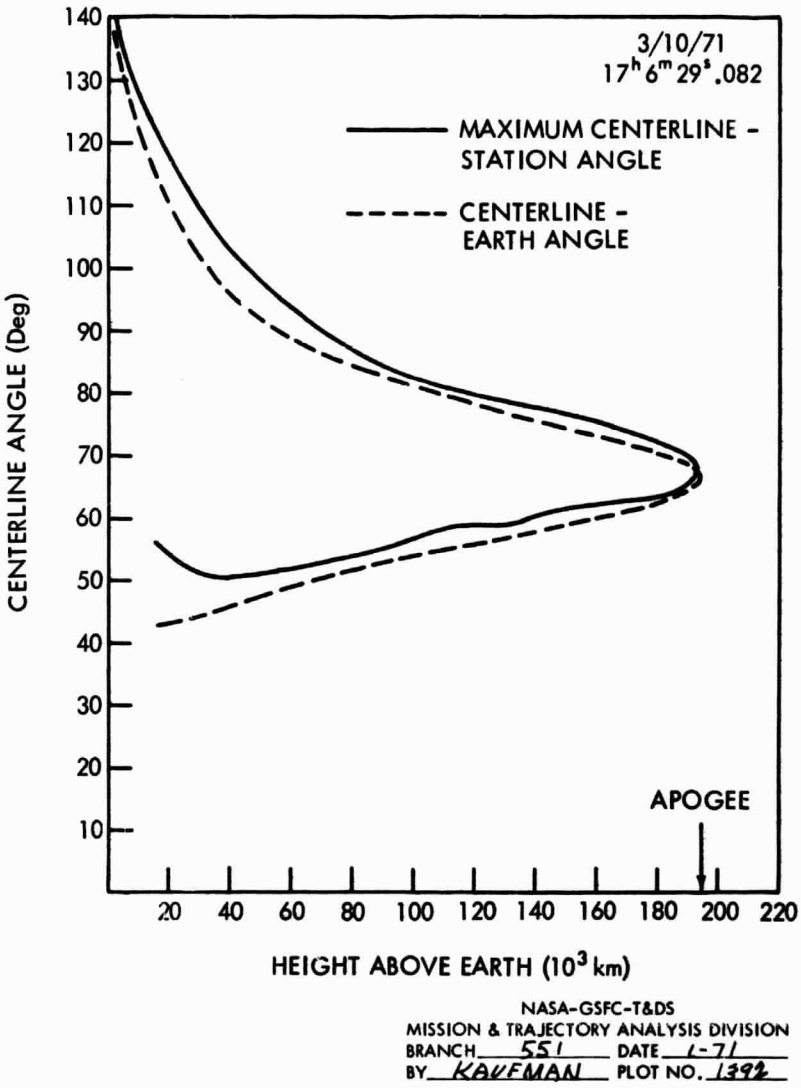

Figure 6. Centerline Angle

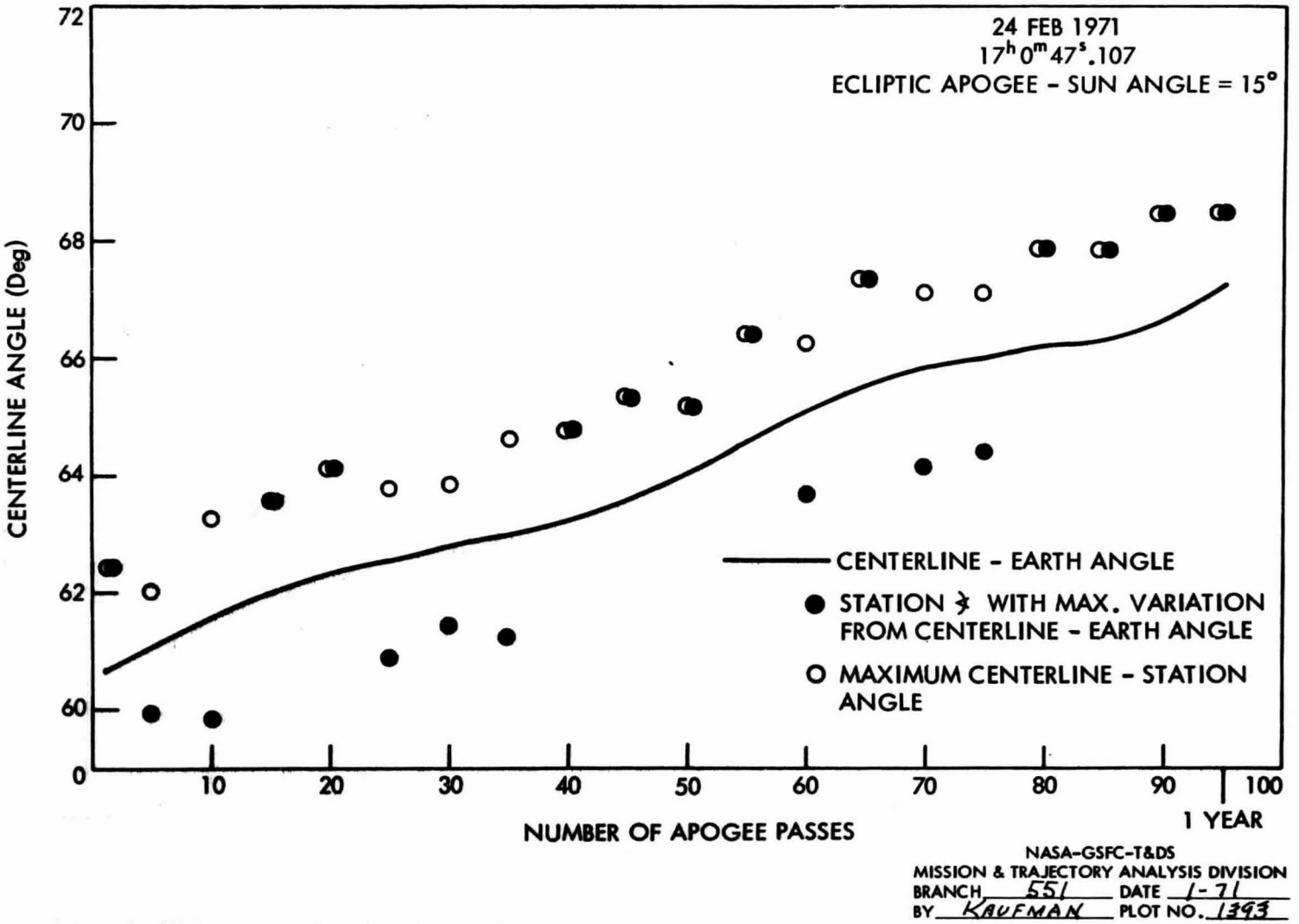

Figure 7. Centerline Angles for One Year

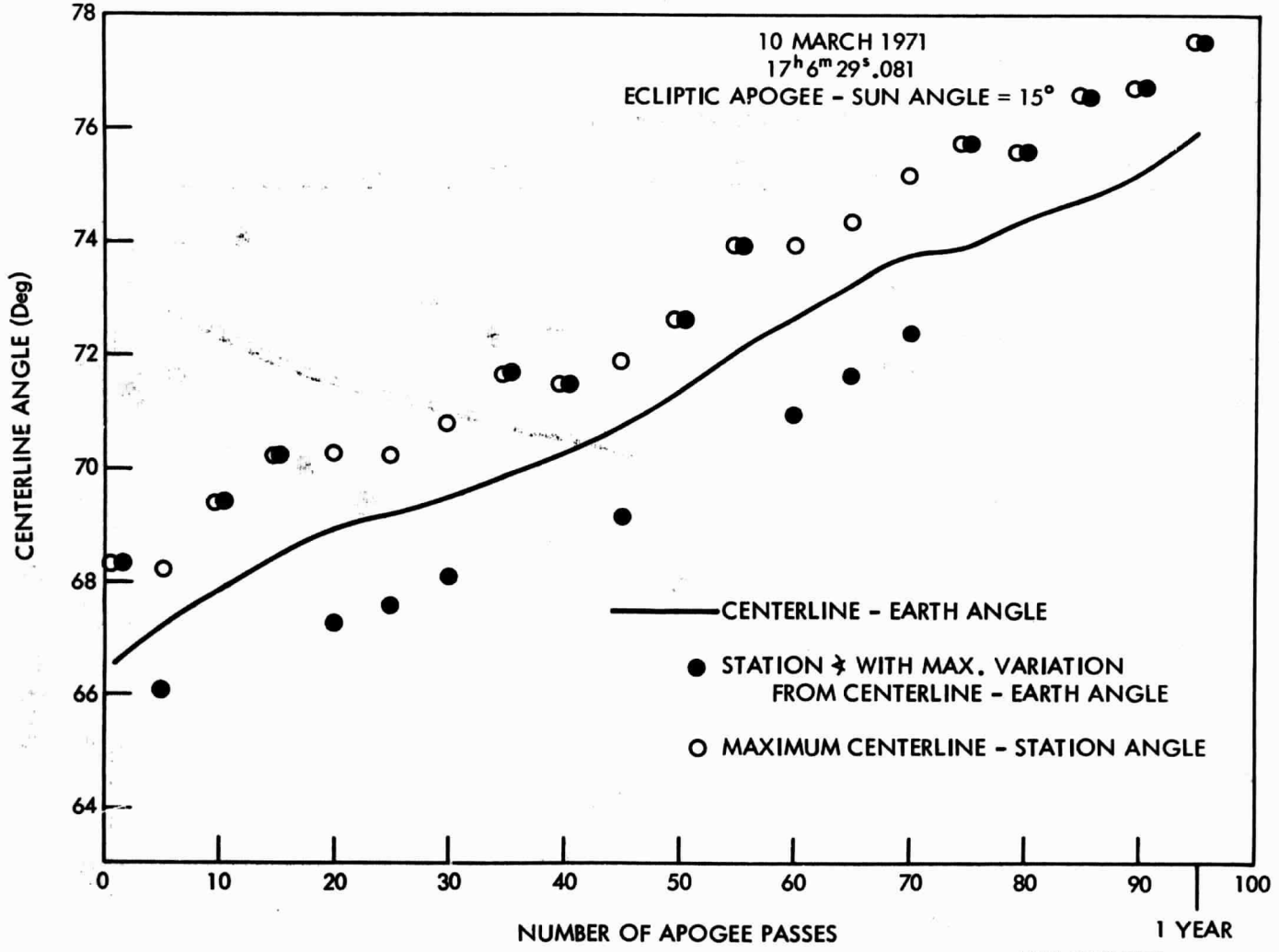

Figure 8: Centerline Angles for One Year

NASA-GSFC-T&DS
MISSION & TRAJECTORY ANALYSIS DIVISION
BRANCH 551 DATE 1-71
BY KAUFMAN PLOT NO. 1394

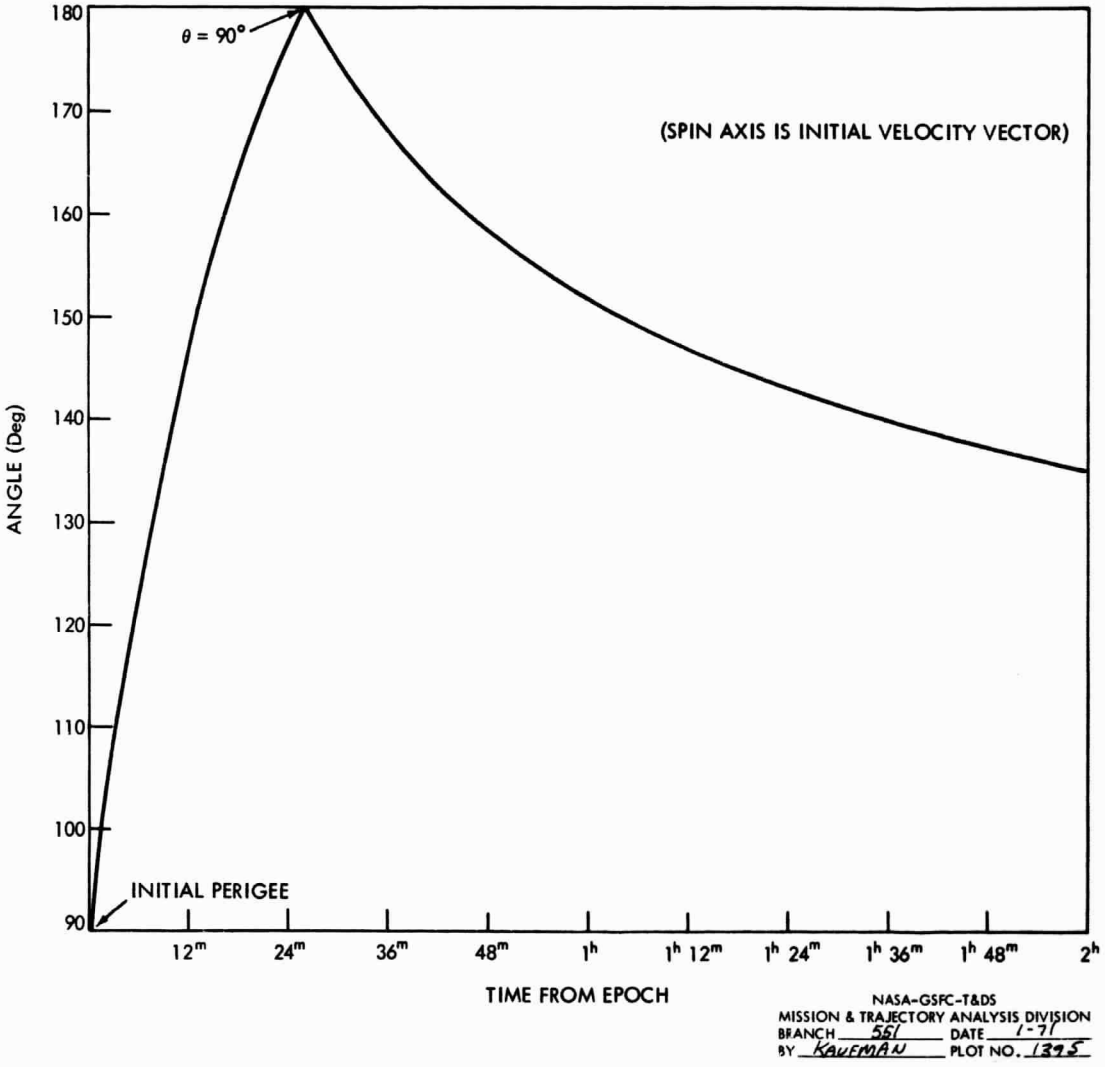

Figure 9. Spin Axis - Earth Angle

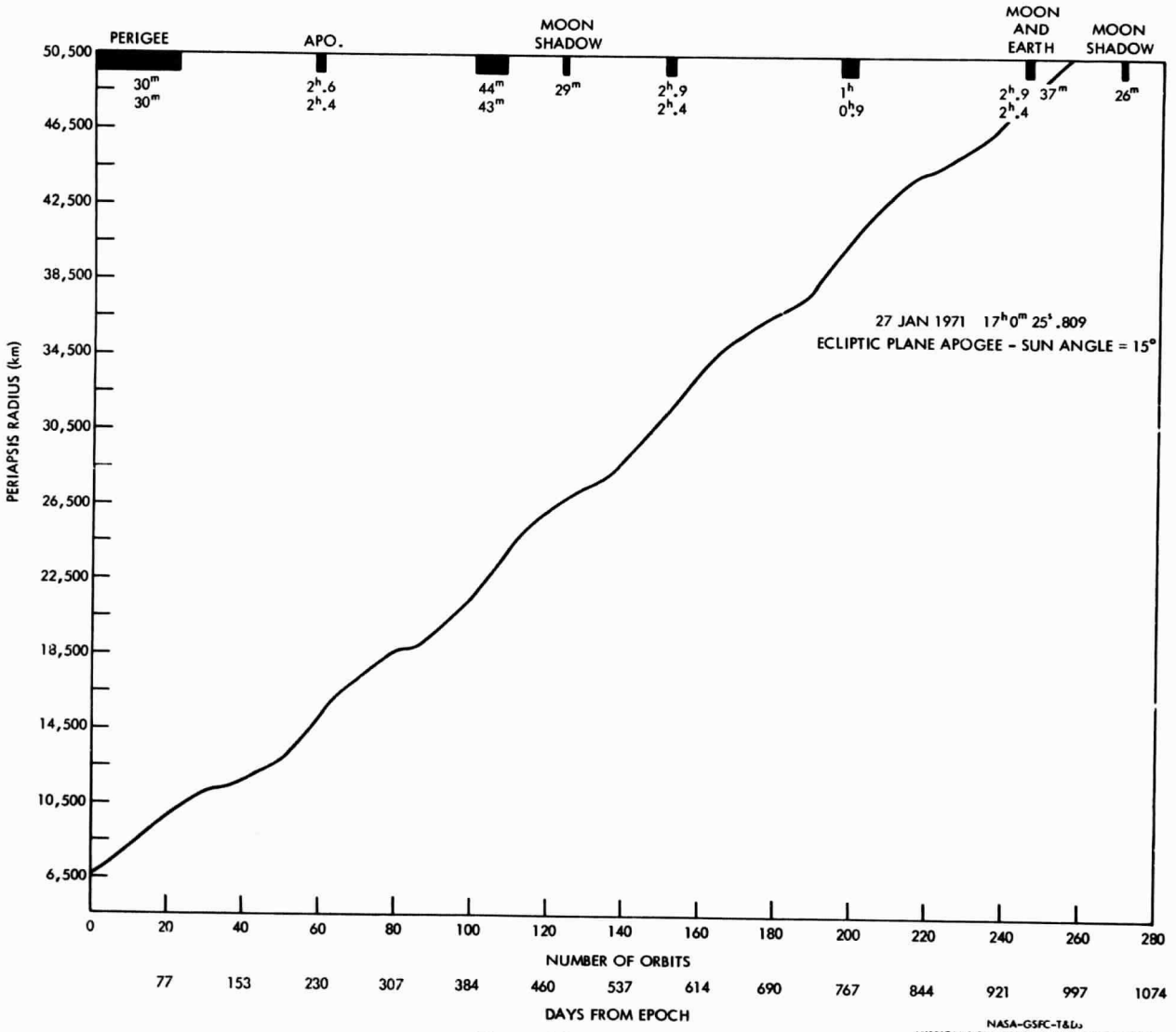

Figure 10.. Perigee vs. Time

NASA-GSFC-T&D
MISSION & TRAJECTORY ANALYSIS DIVISION
BRANCH 551 DATE 1-71
BY KAVEMAN PLOT NO. 1396

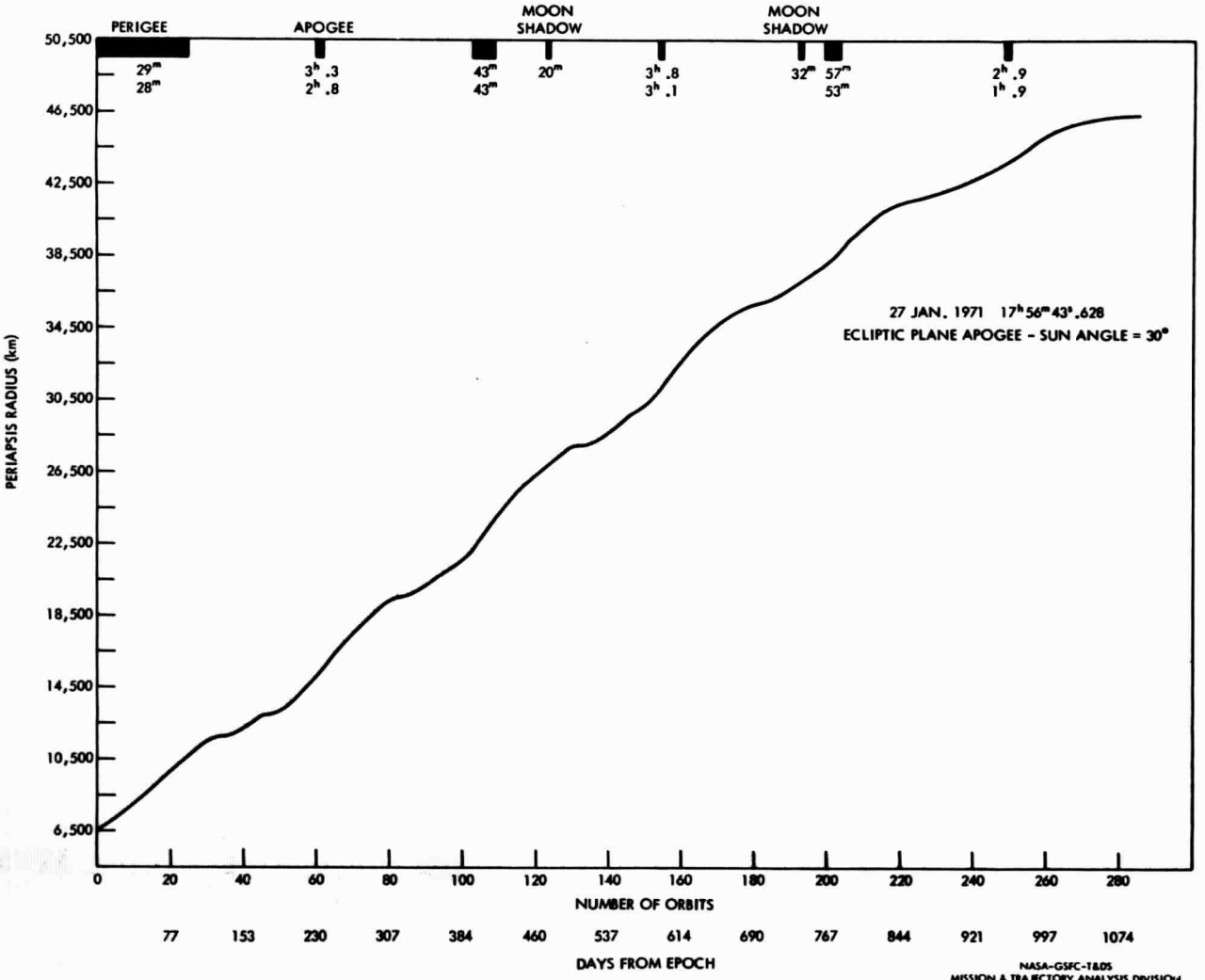

Figure 11. Perigee vs. Time

NASA-GSFC-T&DS
MISSION & TRAJECTORY ANALYSIS DIVISION
BRANCH 551 DATE 1-71
BY KAUFMAN PLOT NO. 1877

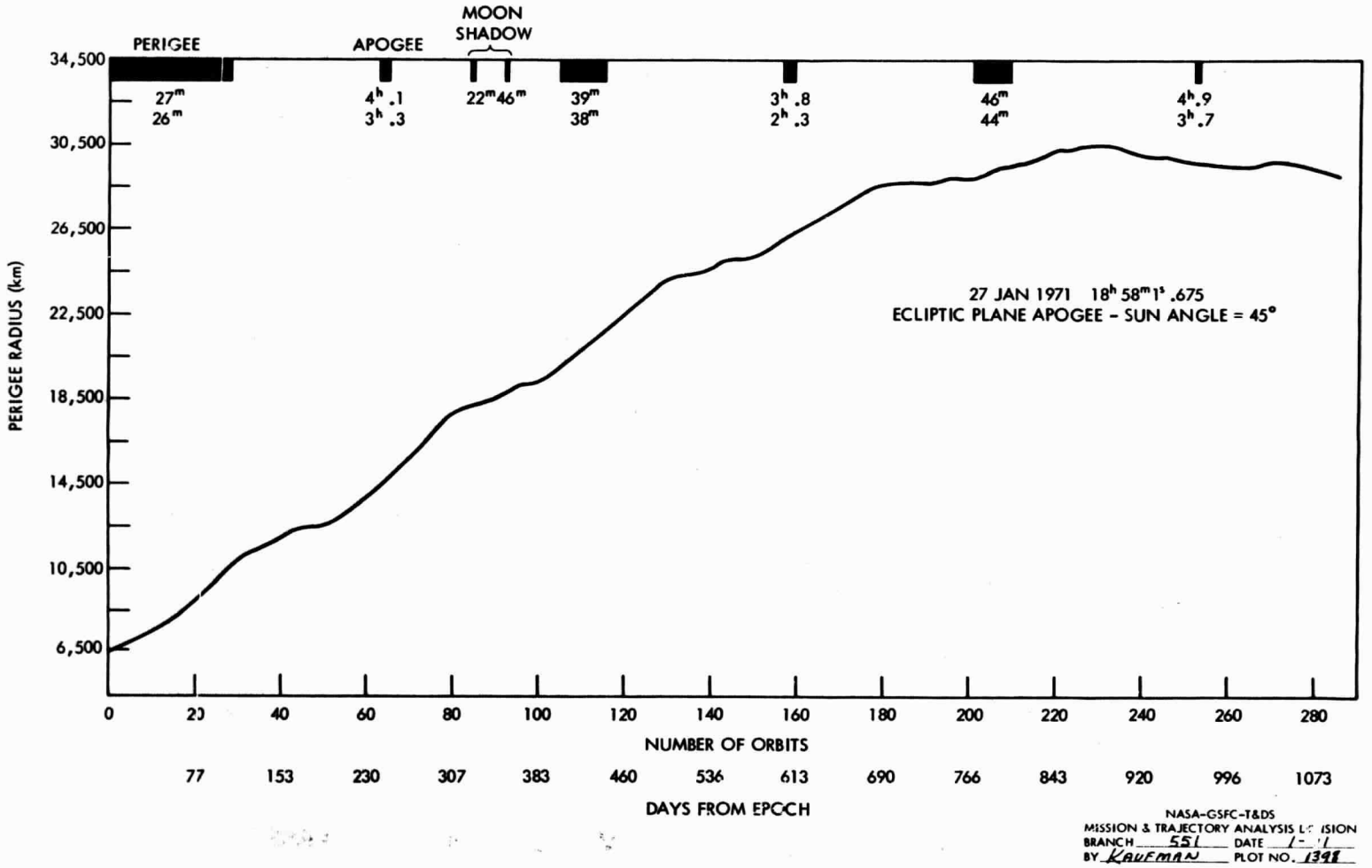

Figure 12. Perigee vs. Time

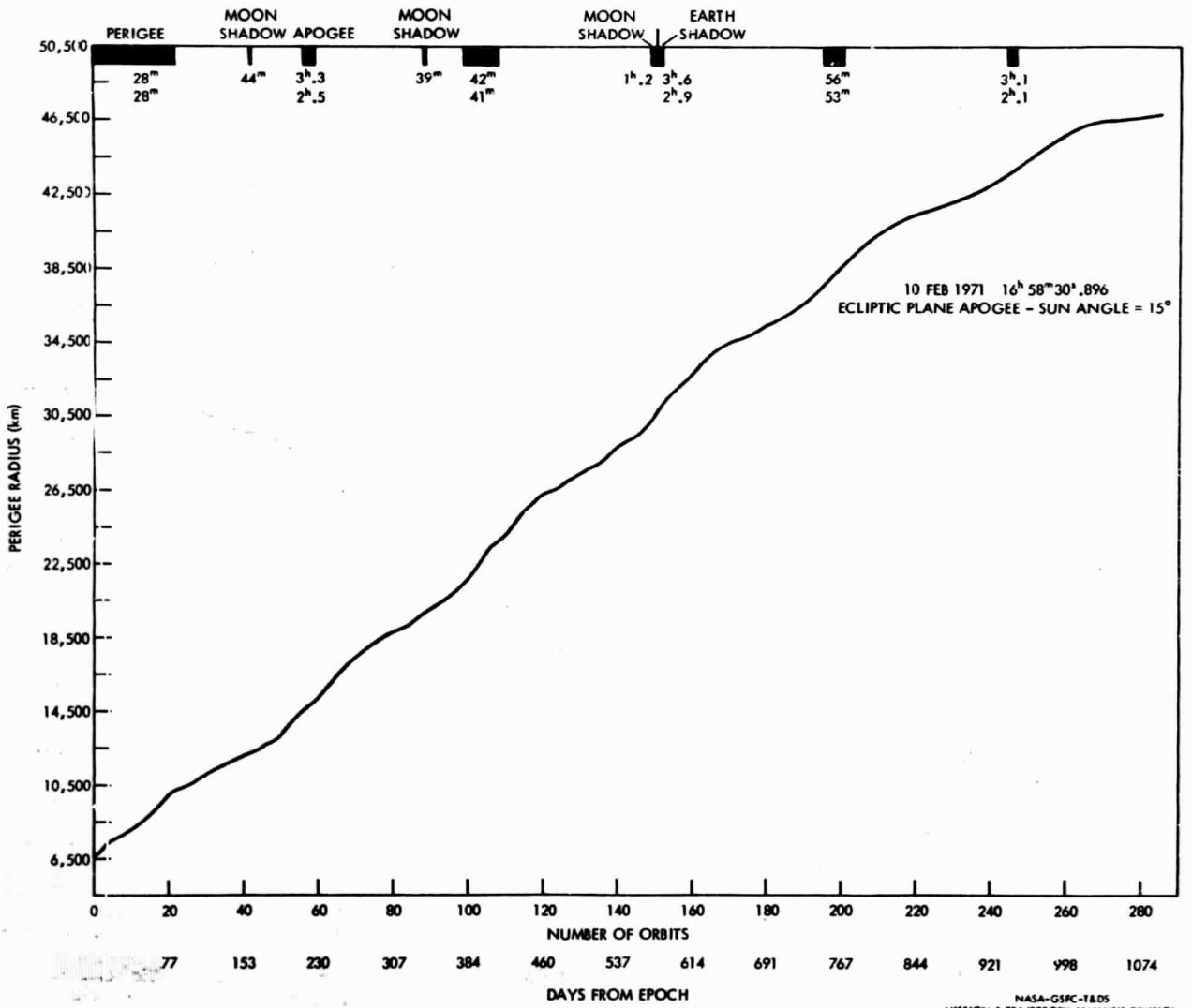

Figure 13. Perigee vs. Time

NASA-GSFC-T&DS
MISSION & TRAJECTORY ANALYSIS DIVISION
BRANCH 551 DATE 1-71
BY Kaufman PLOT NO. 1799

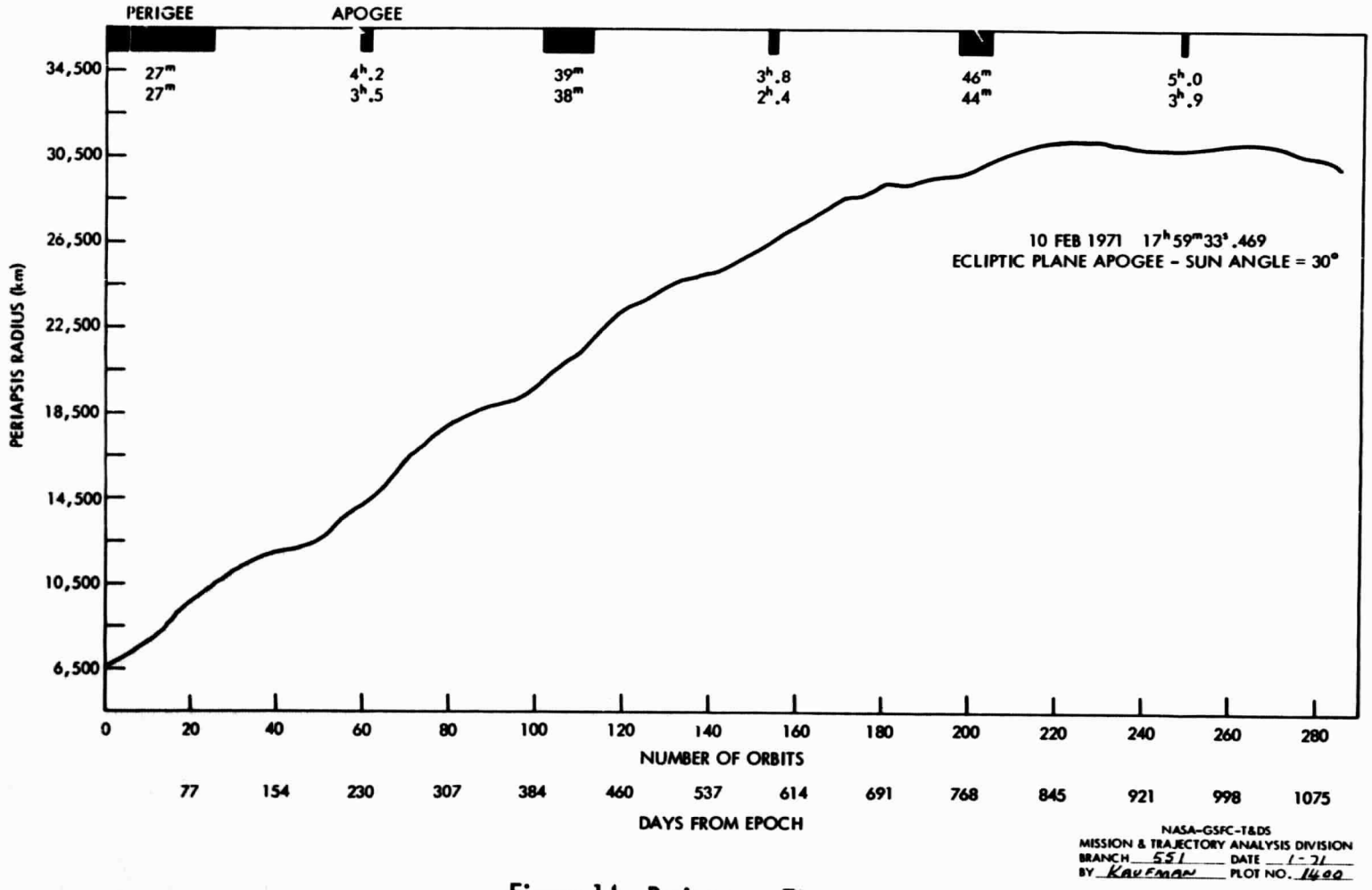

Figure 14. Perigee vs. Time

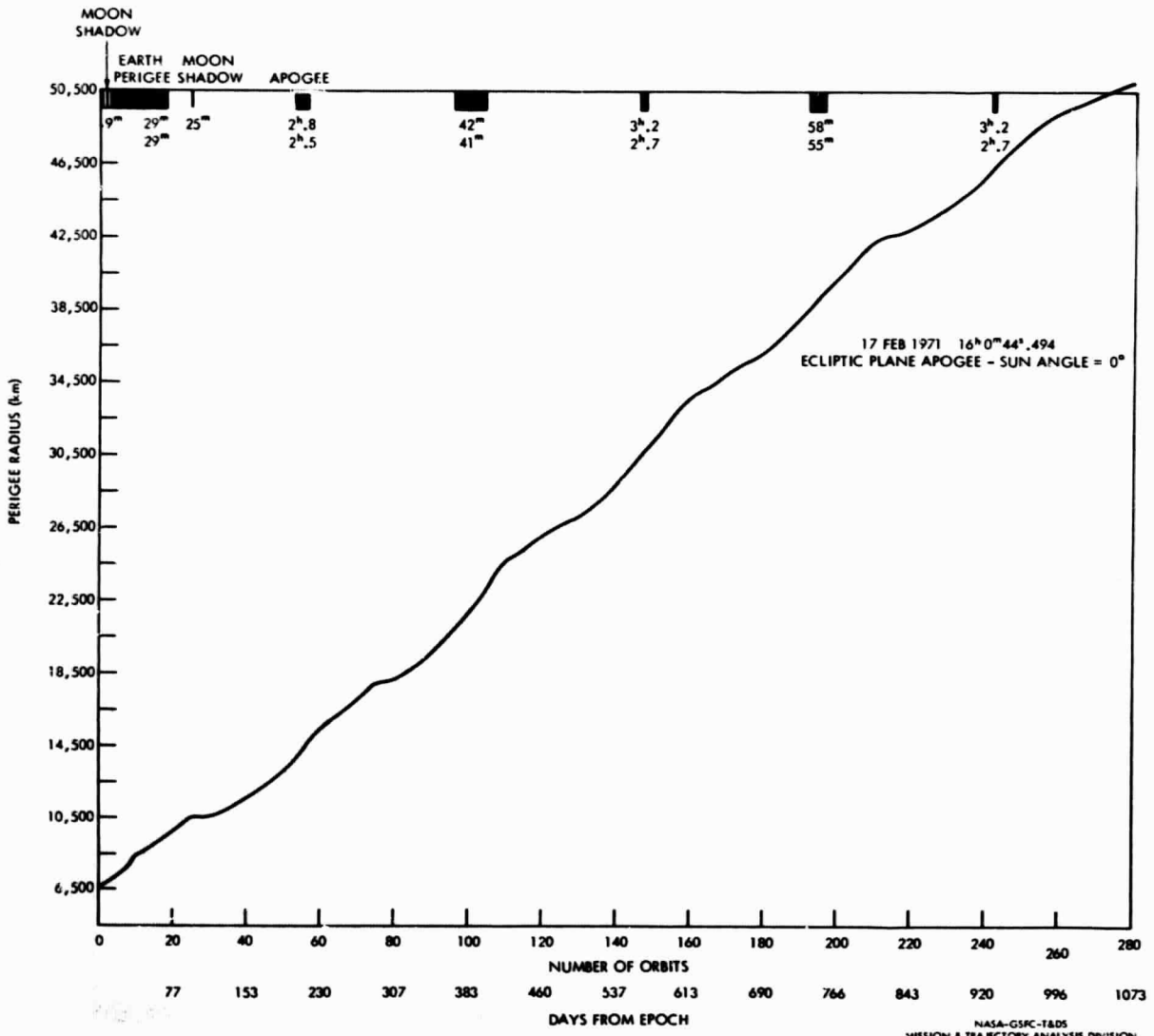

Figure 15. Perigee vs. Time

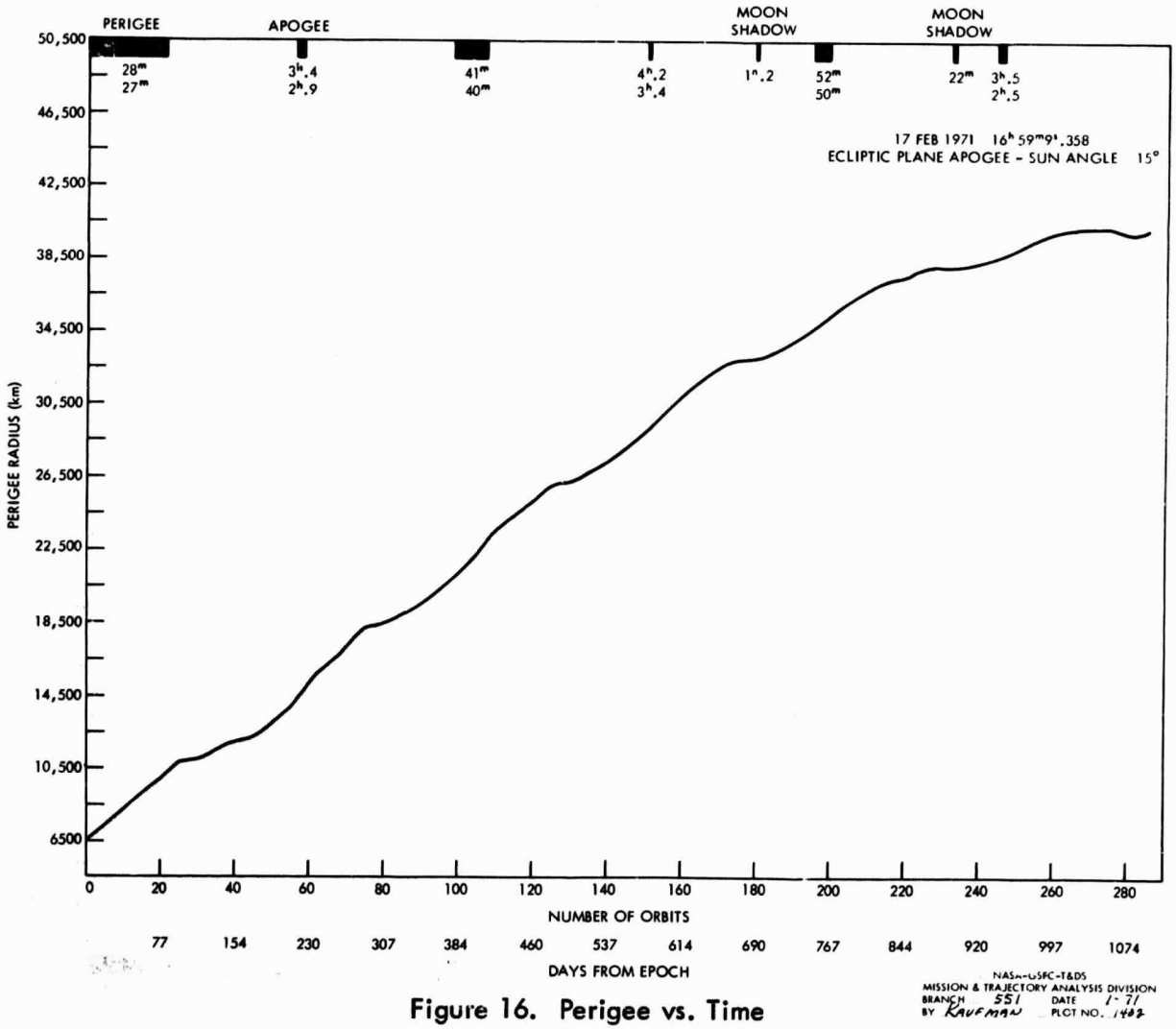

Figure 16. Perigee vs. Time

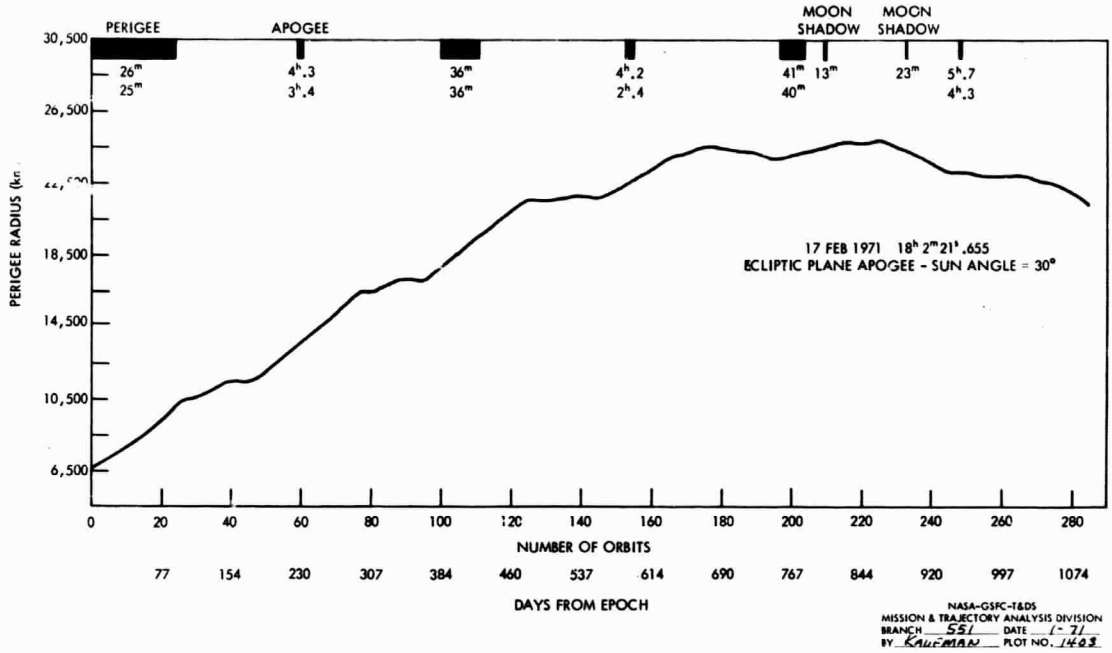

Figure 17. Perigee vs. Time

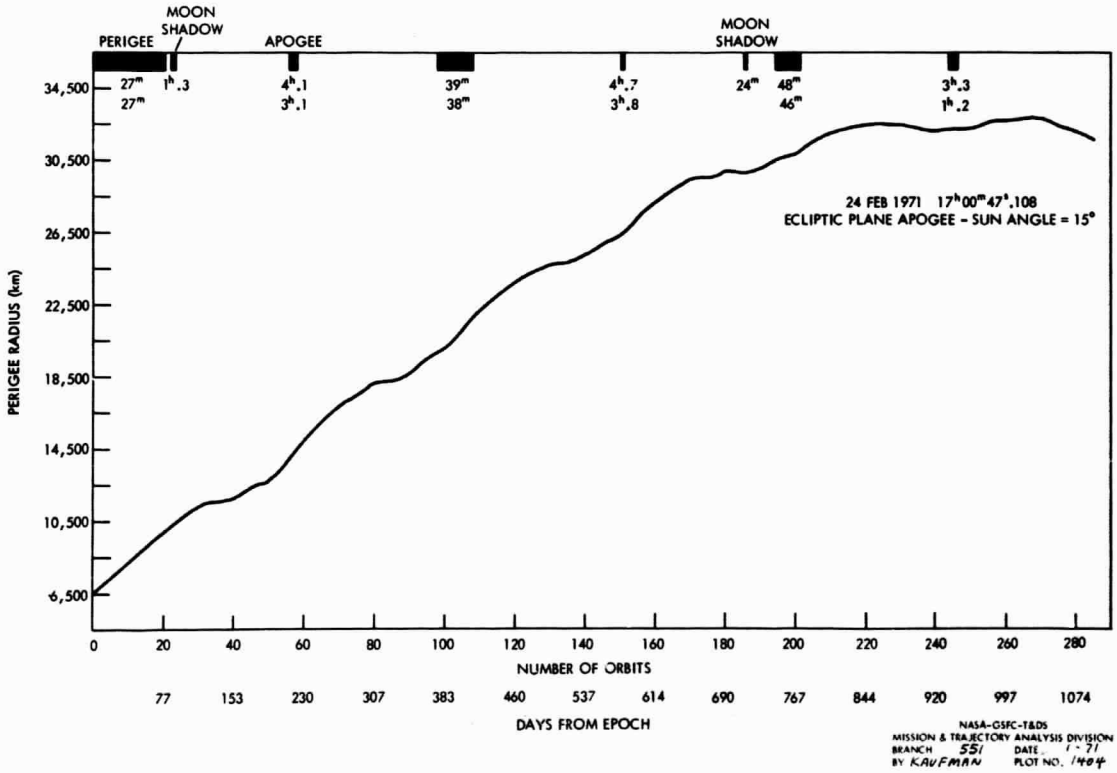

Figure 18. Perigee vs. Time

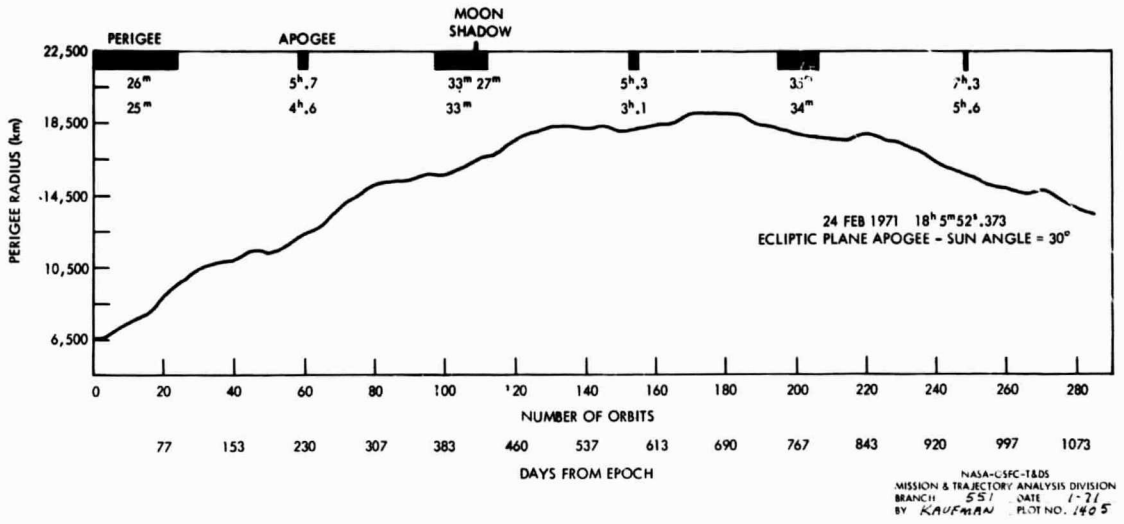

Figure 19. Perigee vs. Time

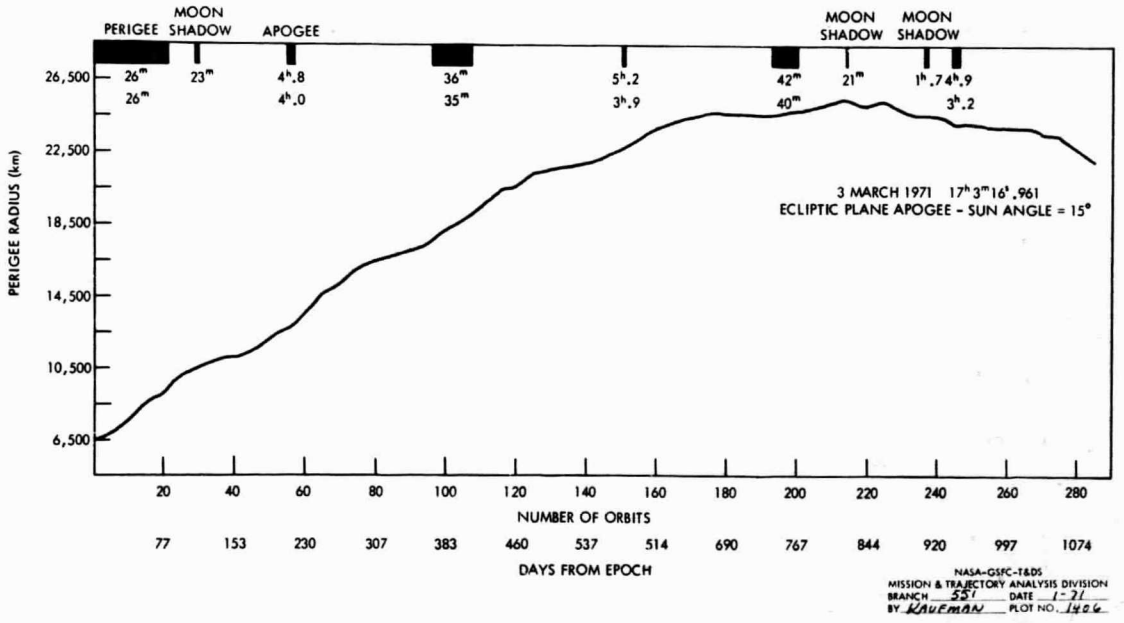

Figure 20. Perigee vs. Time

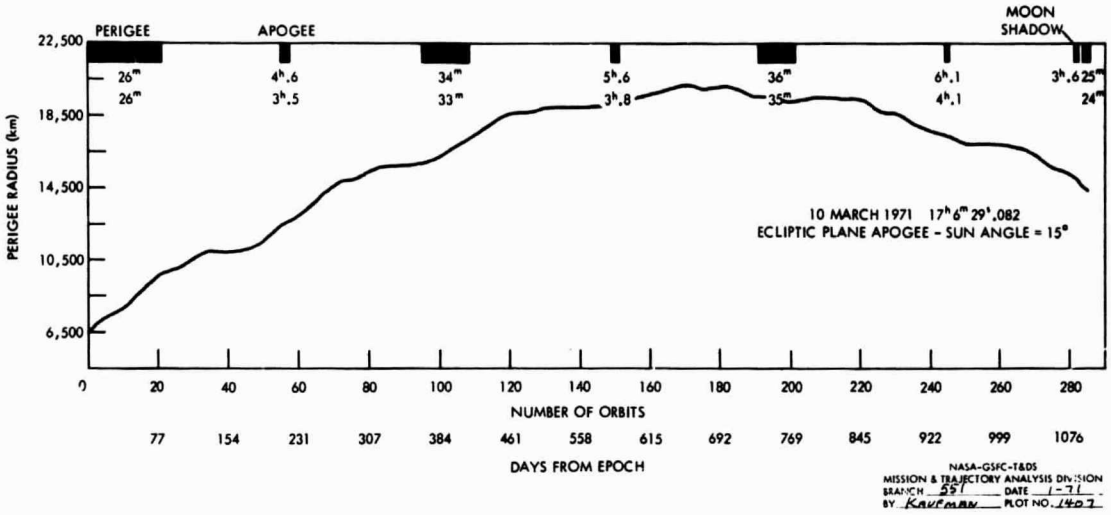

Figure 21. Perigee vs. Time

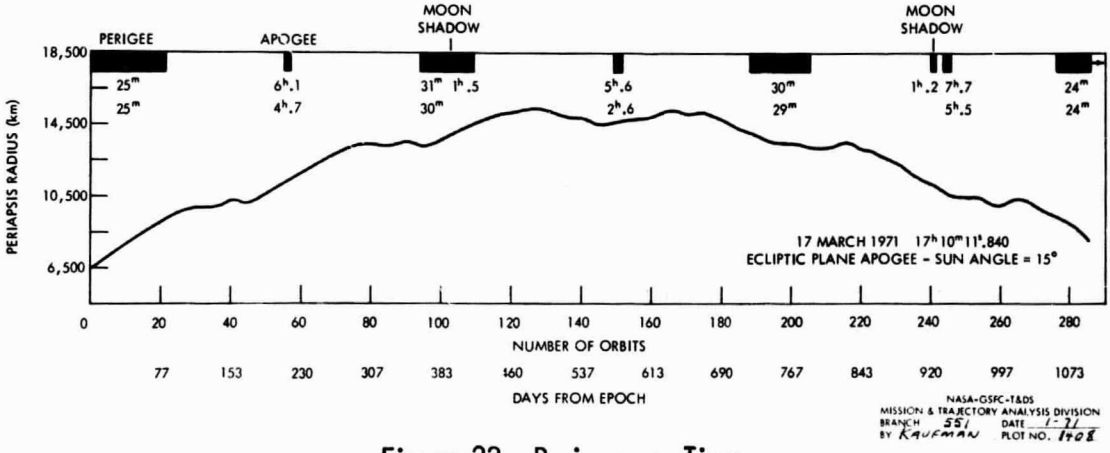

Figure 22. Perigee vs. Time

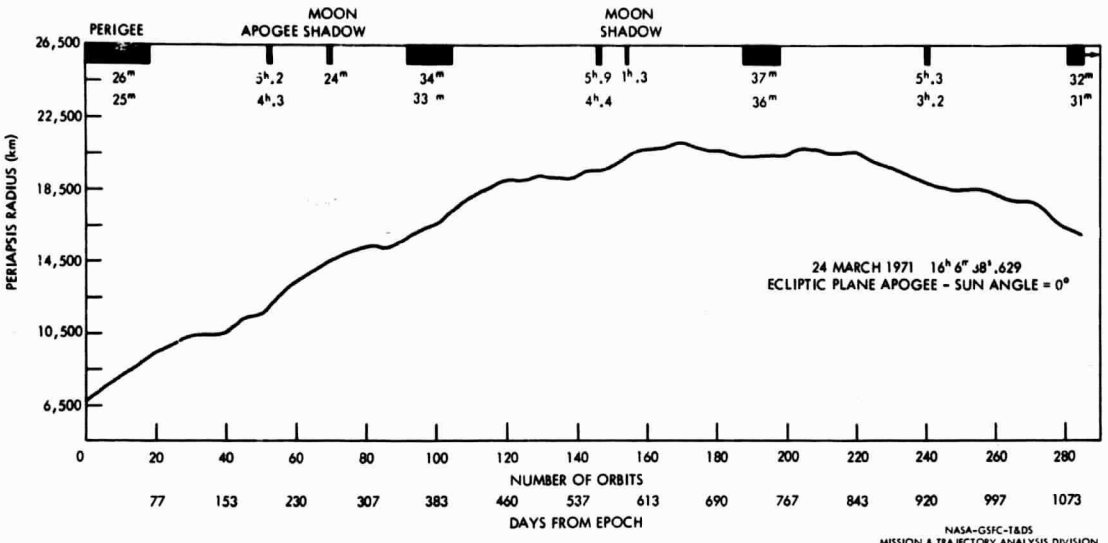

Figure 23. Perigee vs. Time

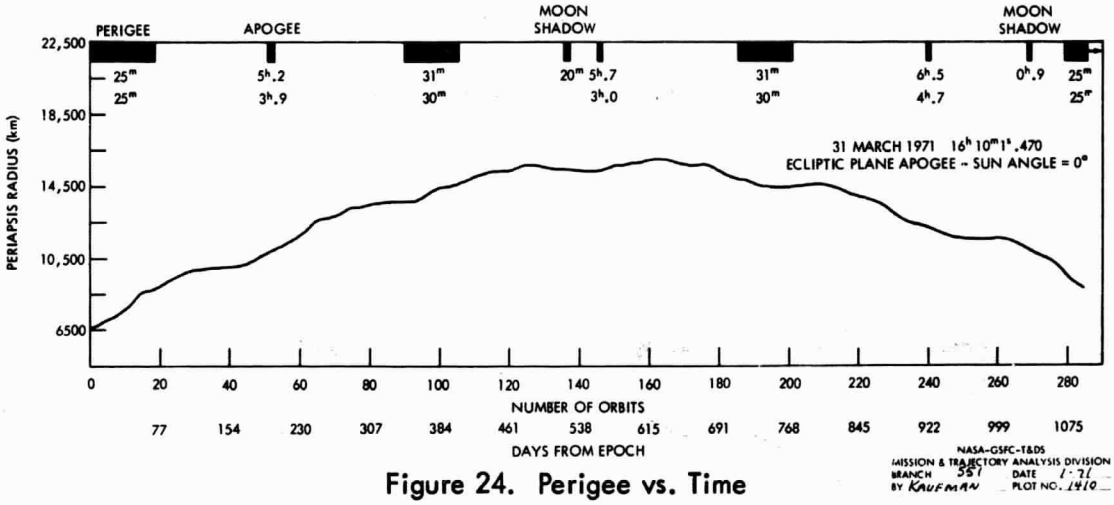

Figure 24. Perigee vs. Time

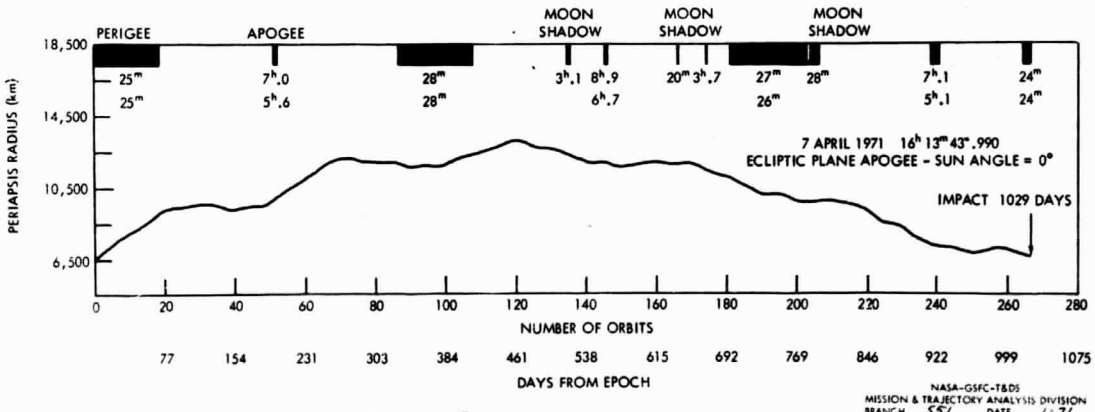

Figure 25. Perigee vs. Time

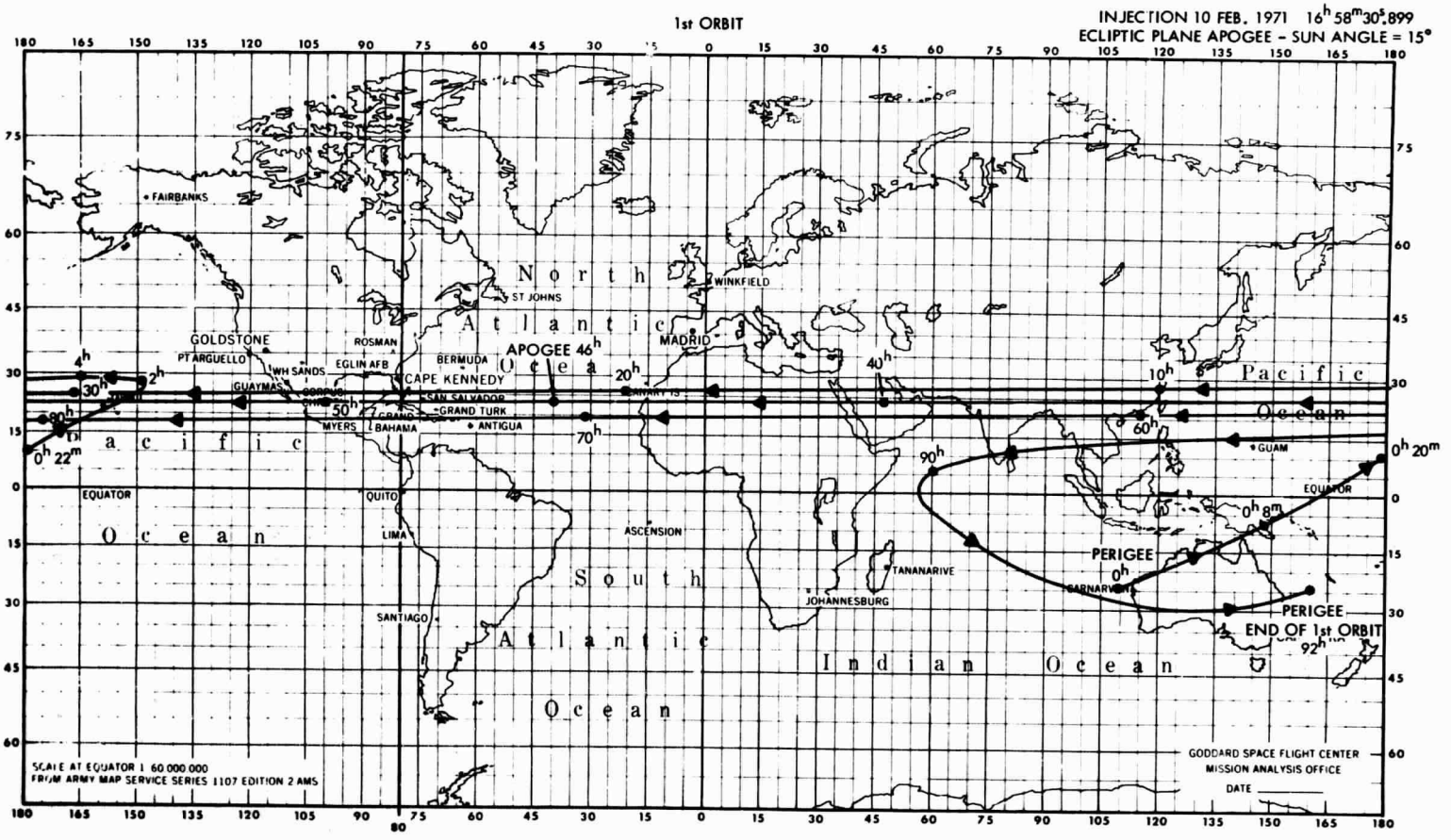

Figure 26. World Map

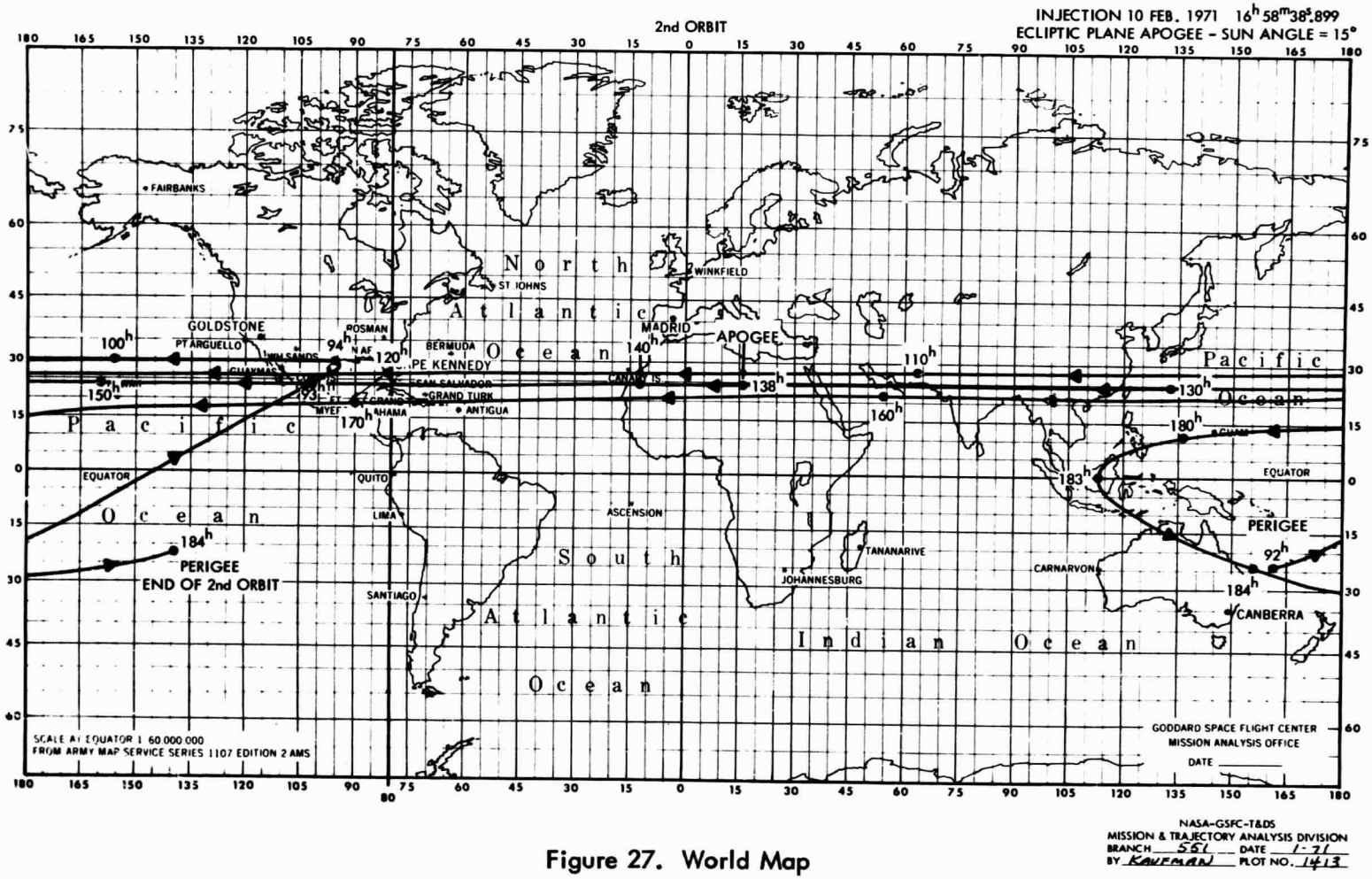

NASA-GSFC-T&DS
MISSION & TRAJECTORY ANALYSIS DIVISION
BRANCH 551 DATE 1-71
BY KAUFMAN PLOT NO. 1413

Figure 27. World Map